The

Geophysical Journal

of the

Royal Astronomical Society

Volume 5 No. 4 October 1961

Published and Sold by the

Royal Astronomical Society

Burlington House, London, W.1, England

Price £1 1s (US$ 3) *Annual Subscription £3 3s (US$ 9)*

The Geophysical Journal

of the Royal Astronomical Society

Editors

A. H. Cook, M.A., Ph.D., F.R.A.S., F.G.S.
(*Geophysical Secretary*)
National Physical Laboratory,
Teddington, Middx.

T. F. Gaskell,
M.A., Ph.D., F.R.A.S.
British Petroleum Company,
London.

The following papers have been accepted for publication:

N. Kawai, Mountain-building movement in Japan and its vicinity.
F. H. Hibberd, An analysis of the position of the Earth's magnetic pole in the geological past.
N. Kawai, H. Ito & S. Kume, Formation of the Japanese arc inferred from rock magnetism.
N. A. Ostenso, Note on the paper of F. F. Evison, C. E. Ingham, R. H. Orr & J. H. Le Fort, "Thickness of the Earth's crust in Antarctica and the surrounding oceans".
D. Van Hilten, A deviating permian pole from rocks in Northern Italy.
A. C. Hamilton, Evaluation of the Dominion Observatory bronze pendulum apparatus.
J. R. Rossiter, Interaction between tide and surge in the Thames.
S. P. Clark, Jr., Heat flow in the Austrian Alps.
G. W. Lennon, The deviation of the vertical at Bidston in response to the attraction of ocean tides.
J. A. Hudson, Love waves in a heterogeneous medium.
K. D. Cole, On solar wind generation of polar geomagnetic disturbance.
K. W. T. Graham, The re-magnetization of a surface outcrop by lighting currents.
H. Jeffreys, Small corrections in the theory of surface waves.
J. A. Miller, K. Shibata & M. Munroe, The potassium–argon age of the lava of Killerton Park, Exeter.
J. A. Miller, The potassium–argon age of the Skiddaw and Eskdale granites.
C. Bull, E. Irving & I. Willis, Further palaeomagnetic results from South Victoria Land.
G. D. Garland & D. H. Lennox, Heat flow in Western Canada.
E. Irving, Palaeomagnetic directions and pole positions, IV.
E. W. Carpenter, R. A. Savill & J. K. Wright, The dependence of seismic signal amplitudes on the size of underground explosions.
G. E. Cook, Luni-solar perturbations of the orbit of an earth satellite.
R. A. Savill, E. W. Carpenter & J. K. Wright, The derivation and solution of indicator equations for seismometer-galvanometer combinations including the effect of seismometer inductance.
C. W. F. Everitt & J. A. Clegg, A new field test of palaeomagnetic stability.
R. L. Wilson, The palaeomagnetic history of a doubly-baked rock.
W. A. Fowler, J. L. Greenstein & F. Hoyle, Nucleosynthesis during the early history of the solar system.
B. A. Bolt & A. Marussi, Eigenvibrations of the Earth observed at Trieste.
W. D. Parkinson, The influence of continents and oceans on geomagnetic variations.
E. C. Bullard, The nature of the Mohorovičić discontinuity.
K. O. Westphal & J. A. Jacobs, Oscillations of the Earth's outer atmosphere and micropulsations.
J. C. Behrendt, R. J. Wold & T. S. Laudon, Gravity base stations in Antarctica.

The Geophysical Journal

of the

ROYAL ASTRONOMICAL SOCIETY

Vol. 5 No. 4 October 1961

The Flow of Water through the Irish Sea and its Relation to Wind

K. F. Bowden and P. Hughes

(Received 1961 January 4)

Summary

The method of studying water movements by measuring the electrical potential produced by the transport of water through the Earth's magnetic field has been applied to flow through the Irish Sea. Continuous readings of these potentials were made between 1954 November and 1958 March on a submarine cable which lies on the sea bed of the North Channel between Portpatrick and Donaghadee. Similar measurements were made further south on a Nevin–Howth cable during the period 1956 December to 1958 March. To calibrate the cable signals, direct current measurements were made at different depths in a number of localities in the North Channel. No measurements were carried out to calibrate the Nevin–Howth cable, however, but an estimate was made from values given in Admiralty publications.

Daily values of the current in the North Channel referred to the long period mean as zero are presented and it is shown that high correlations existed during the winter months between these flows and the regional winds. During the summer, however, the correlation was not as strong. Linear regression equations relating the mean flow to the regional wind were computed for bi-monthly, six-monthly and total periods. The results showed that a wind from S 49° E was the most effective in producing a transport of water northwards through the North Channel and that under these conditions the flow amounted to about 1 per cent of the wind speed. Furthermore, estimates of the accumulated transport of water due to the wind, suggest that the mean flow over a long period deduced from the salinity distribution may be due almost entirely to the residual effect of the wind. From consideration of a current surge on 1955 November 2 it is shown that the flow lagged behind the generating wind by only about two hours.

The Geophysical Journal
of the Royal Astronomical
Society

Editors

A. H. Cook, M.A., Ph.D., F.R.A.S., F.G.S.
(*Geophysical Secretary*)
National Physical Laboratory,
Teddington, Middx.

T. F. Gaskell,
M.A., Ph.D., F.R.A.S.
British Petroleum Company,
London.

The following papers have been accepted for publication:

N. Kawai, Mountain-building movement in Japan and its vicinity.

F. H. Hirasawa, An analysis of the position of the Earth's magnetic pole in the geological past.

N. Kawai, H. Fuji & S. Kuno, Formation of the Japanese arc inferred from rock magnetism.

N. A. Ostenso, Note on the paper of F. F. Evison, C. E. Ingham, R. H. Orr & J. H. Le Fort, "Thickness of the Earth's crust in Antarctica and the surrounding oceans".

D. Van Hilten, A deviating permian pole from rocks in Northern Italy.

A. C. Hamilton, Evaluation of the Dominion Observatory bronze pendulum apparatus.

J. K. Rossiter, Interaction between tide and surge in the Thames.

S. P. Clark, Jr., Heat flow in the Austrian Alps.

G. W. Lennon, The deviation of the vertical at Bidston in response to the attraction of ocean tides.

J. A. Hudson, Love waves in a heterogeneous medium.

K. D. Cole, On solar wind generation of polar geomagnetic disturbance.

K. W. T. Graham, The re-magnetization of a surface outcrop by lightning currents.

H. Jeffreys, Small corrections in the theory of surface waves.

J. A. Miller, K. Shibata & M. Muroor, The potassium-argon age of the lava of Killerton Park, Exeter.

J. A. Miller, The potassium-argon age of the Skiddaw and Eskdale granites.

C. Doll, E. Irving & I. Willis, Further palaeomagnetic results from South Victoria Land.

G. D. Garland & D. H. Lennox, Heat flow in Western Canada.

E. Irving, Palaeomagnetic directions and pole positions, IV.

E. W. Carpenter, J. A. Savill & J. K. Wright, The dependence of seismic signal amplitudes on the size of underground explosions.

G. E. Cook, Luni-solar perturbations of the orbit of an earth satellite.

E. A. Savill, E. W. Carpenter & J. K. Wright, The derivation and solution of indicator equations for seismometer-galvanometer combinations including the effect of seismometer inductance.

C. W. F. Everitt & J. A. Clegg, A new field test of palaeomagnetic stability.

R. L. Wilson, The palaeomagnetic history of a doubly-baked rock.

W. A. Fowler, J. L. Greenstein & F. Hoyle, Nucleosynthesis during the early history of the solar system.

B. A. Bolt & A. Marussi, Eigenvibrations of the Earth observed at Trieste.

W. D. Parkinson, The influence of continents and oceans on geomagnetic variations.

E. C. Bullard, The nature of the Mohorovičić discontinuity.

K. G. Westphal & J. A. Jacobs, Oscillations of the Earth's outer atmosphere and micropulsations.

J. C. Behrendt, R. J. Wold & T. S. Lemmon, Gravity base stations in Antarctica.

The Geophysical Journal

of the

ROYAL ASTRONOMICAL SOCIETY

Vol. 5 No. 4 October 1961

The Flow of Water through the Irish Sea and its Relation to Wind

K. F. Bowden and P. Hughes

(Received 1961 January 4)

Summary

The method of studying water movements by measuring the electrical potential produced by the transport of water through the Earth's magnetic field has been applied to flow through the Irish Sea. Continuous readings of these potentials were made between 1954 November and 1958 March on a submarine cable which lies on the sea bed of the North Channel between Portpatrick and Donaghadee. Similar measurements were made further south on a Nevin–Howth cable during the period 1956 December to 1958 March. To calibrate the cable signals, direct current measurements were made at different depths in a number of localities in the North Channel. No measurements were carried out to calibrate the Nevin–Howth cable, however, but an estimate was made from values given in Admiralty publications.

Daily values of the current in the North Channel referred to the long period mean as zero are presented and it is shown that high correlations existed during the winter months between these flows and the regional winds. During the summer, however, the correlation was not as strong. Linear regression equations relating the mean flow to the regional wind were computed for bi-monthly, six-monthly and total periods. The results showed that a wind from S 49°E was the most effective in producing a transport of water northwards through the North Channel and that under these conditions the flow amounted to about 1 per cent of the wind speed. Furthermore, estimates of the accumulated transport of water due to the wind, suggest that the mean flow over a long period deduced from the salinity distribution may be due almost entirely to the residual effect of the wind. From consideration of a current surge on 1955 November 2 it is shown that the flow lagged behind the generating wind by only about two hours.

Correlation of the Portpatrick and Nevin records confirmed the occurrence of periods of wind induced flow through the Irish Sea as a whole. Uncertain changes in the zero of each cable, which were probably attributable to Earth currents, prevented a study being made of the water balance.

1. Introduction

It is known from the salinity distribution that, over a long period, there is a net flow of water through the Irish Sea from south to north. The mean velocity through the North Channel was estimated by Knudsen (1907), from considerations of continuity, to be 1·9 km/day. A more detailed calculation by the same method (Bowden 1950) indicated that a large part of the exchange of salt content through the North Channel was probably due to longitudinal mixing and that the mean flow was only about 0·5 km/day. This flow, small as it is, is much larger than the displacement current needed to remove the fresh water added to the sea by rainfall and run-off, which would be of the order of 0·02 km/day.

Current measurements at mid-depth were made at the Skulmartin light-vessel, in the North Channel about 3·7 km from the Irish coast, in 1935–36 using a Carruthers drift meter (Proudman 1939). Over a year the residual current was 0·6 km/day towards the south-east, suggesting that the flow at this point was not representative of that across the whole cross-section of the Channel. Individual monthly mean flows were sometimes north-westerly and at other times south-easterly, with maxima of 4 km/day in either direction. Further measurements at the Skulmartin light-vessel, made during a 15-month period in 1953–4 with a Carruthers vertical log current meter, gave similar results.* There was only a poor correlation between the monthly residuals of current and wind.

Other evidence that a southerly flow through the North Channel occurs near the Irish Coast, at least on some occasions, was provided by drift bottle results reported by Tait (1952). Drift bottles released within the Irish Sea in a number of investigations (e.g. Daniel & Lewis 1929) have shown that the drift of the surface water is variable and is determined mainly by the wind. The results have also given some indication, however, of a general northerly flow superimposed on the wind drift. Williamson (1956) discussed the value of various species of plankton as indicators of water movements in the Irish Sea and concluded that, in general, they confirmed the pattern of flow outlined above.

The cable method of measuring flow through a channel makes use of the electromotive force induced in the water by its movement through the Earth's magnetic field. The potential difference across the channel is proportional to the mean velocity of the water across the whole cross-section. In 1953–54 a study was made of the flow of water through the Straits of Dover by this method (Bowden 1956). The recorded values of flow were correlated with the wind, which influenced the flow directly by its tangential stress on the surface of the water and indirectly by causing a piling up of water due to the constriction of the English Channel in the region of the Straits of Dover. The resultant slope of the sea surface gave rise to a component of flow.

In the present investigation, the same method was applied to the flow through the North Channel, using a suitably located telephone cable. As in the case of the Straits of Dover, the voltage recorded on the cable was calibrated in terms of

* Unpublished data, supplied by Cdr. A. L. Lawford, National Institute of Oceanography.

measured values of the tidal currents. To study the non-tidal flow, the tidal currents were eliminated and the residual flow across the section correlated with the wind over the area. The information obtained in such an investigation is of interest in connection with the exchange of water between the Irish Sea and the region outside the North Channel.

2. Apparatus

The observations in the North Channel were made on a telephone cable running from Portpatrick, Scotland, to Donaghadee, Northern Ireland, which was put at our disposal by the Post Office. The recording gear was housed in the telephone repeater station at Portpatrick. Records were obtained covering the period from 1954 November to 1958 March. For a part of this period, observations were also made on a cable running from Nevin, North Wales, to Howth, Eire. The positions of the cables are shown in Figure 1, and profiles of the sea bed across the channel at each location are shown in Figures 2(a) and 2(b).

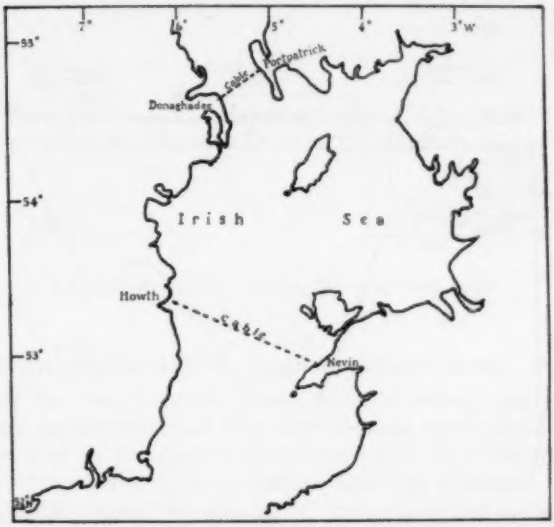

FIG. 1.—Irish Sea and the cable positions.

The recording circuits at Portpatrick and Nevin. At Portpatrick the measurements were made on a reserve four-core submarine cable running from a point about two miles north of Portpatrick, Scotland, to Donaghadee, Northern Ireland. The circuit arrangements are shown in Figure 3.

A phantom circuit was used as the return path for the water induced signal, the connections being taken from the centre point of the cable side of the line transformers associated with a side circuit. The sea earth referred to in the diagram is the unprotected cable sheath which acts as a continuous electrode across the channel.

A siphon-pen recording milliammeter, having a full scale deflection of 1 mA and a nominal internal resistance of 1000 Ω was used to measure the varying cable potentials. The instrument was of the centre zero type so that the ebb and flow of the tide were recorded as positive and negative movements of the pen across the paper. The chart speed was constant at 1 inch per hour, and this was adequate for the investigation. When the system was being set up resistances in the control

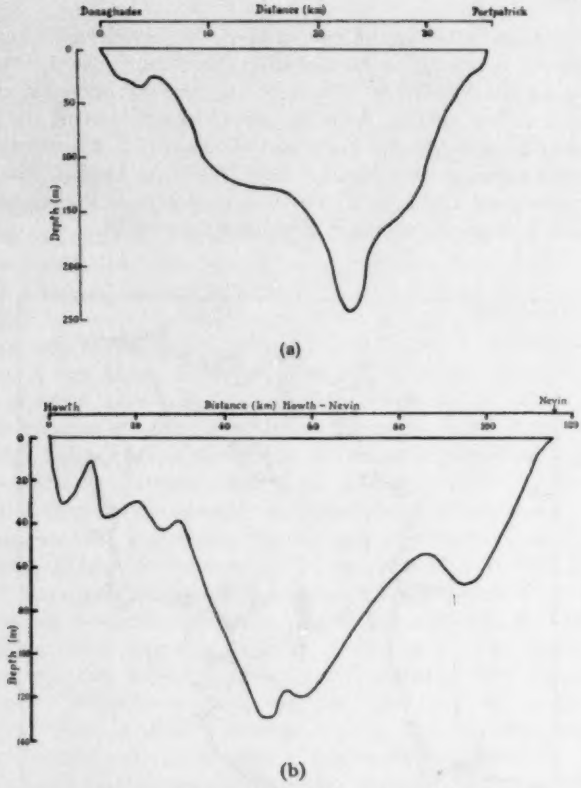

FIG. 2.—Profiles of the sea bed across the channel at each cable location. (a) North Channel (Portpatrick–Donaghadee cable). (b) St George's Channel (Nevin–Howth cable).

circuit were adjusted so that deflections at tidal springs would traverse most of the width of the recording paper. Twice a week a standardizing signal was applied to indicate an accurate zero and as a functional test of the recorder. The timing of the chart drive was also watched carefully and time marks were placed on the record to allow a comparison of the Portpatrick and Nevin records to be made.

On the cable further south between Nevin in North Wales, and Howth in the Republic of Ireland, a similar set-up with slight modifications was used. The cables available did not terminate at the beach, but were brought straight to the repeater station at 1·2 miles from the shore, and as a result the sheath of the cable

was exposed to land earth connection for that distance. A block schematic diagram of the cable layout is shown in Figure 4.

On the office side of the low pass filter at Nevin a blocking condenser, C, ($8\,\mu$F) is fitted to prevent the d.c. flow from saturating the transformer windings. It was across this condenser, at A–B, that the recording device, similar to the one used at Portpatrick, was connected. As mentioned, a reserve submarine cable was used at Portpatrick, but at Nevin the cable was carrying telephone traffic during the time that recordings were being made.

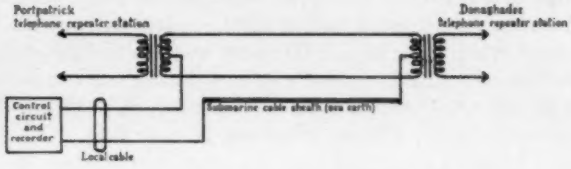

FIG. 3.—Recording circuit, Portpatrick–Donaghadee cable.

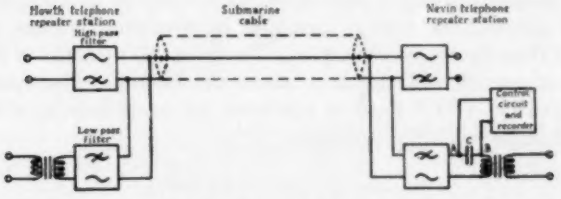

FIG. 4.—Recording circuit, Nevin–Howth cable.

3. Earth currents associated with magnetic disturbances

For most of the time fluctuations of a variable nature, both in period and amplitude, were superimposed on the water induced cable signal. These extra variations were due to the earth currents associated with disturbances of the Earth's magnetic field, and their occurrence has been discussed by one of the authors in a previous paper (Bowden 1956). It is interesting to notice, however, the widespread nature of these disturbances, which occurred regularly in the same form on both the Nevin–Howth and the Portpatrick–Donaghadee cables. A typical example is given in Figure 5, where the two records are shown side by side. There is an obvious correspondence between the sets of fluctuations which resemble one another in detail.

There were no recognizable time lags between similar magnetic disturbances recorded at Portpatrick and Nevin. When they were suspected, investigations showed that one or other of the recorder clocks were in error. This aspect, however, was not examined extensively, but the recognizable features always provided a check on the record positions.

The Nevin cable is longer than the Portpatrick cable while the mean depth over the section is less, and this results in relatively stronger disturbances in the

Nevin to Howth cable. The fluctuations are, however, mainly of fairly short period and can easily be removed. Where there was any doubt about this elimination the record was not included in the results. There were, of course, occasional magnetic storms when analysis of the trace was impossible (see Figure 6), but for most of the time the disturbances were small and a good record is shown for comparison. No attempt has been made to analyse the magnetic fluctuations, they were merely removed from the record.

4. Calibration of north channel cable records

The calibration was carried out in terms of the tidal currents, by comparing the observed voltage on the cable record with measurements of the tidal currents made at the same time. Two sets of data were used: (a) Observations by H.M.S. *Cook*, at a position in the centre of the channel, during one complete tidal period on 1955 May 26; (b) Observations with drifting drogues, at three positions across the channel, using the M.V. *William Herdman*, in 1956 July.

(a) *Current measurements by H.M.S. Cook*

The observations were made with a 30 ft drifting pole logship, noting the speed and average direction of current over 30-minute intervals throughout the tidal cycle. The current reached a peak of 2·2 kt (113 cm/s) in each direction. The cable record showed the voltage reaching its maximum values approximately 30 min earlier than the observed current. There was no evidence at this time about the variation of current with depth or across the channel. Assuming the current values measured by H.M.S. *Cook* to represent the mean velocity across the whole section, the calibration factor would be

$$1 \text{ volt} = 3{\cdot}23 \text{ kt } (166 \text{ cm/s}).$$

This gives an upper limit to the current, since the mean velocity across the whole section is almost certainly less than that in the upper 30 ft in the centre of the channel.

(b) *Drifting drogues, observed from M.V. William Herdman*

Each drogue was in the form of two steel plates intersecting at right angles, of overall dimensions 3 ft × 2 ft. The drogue was suspended by steel wire of diameter 0·075 in. from an elliptical buoy of horizontal diameter 14 in and height 10 in. Attached to the buoy was a bamboo cane 10 ft high, carrying a flag of distinctive colour to mark it. Three drogues were normally released together, at depths of 5, 25 and 50 fm (9, 46 and 91·5 m) or 5, 50 and 100 fm (9, 91·5 and 183 m).

If the velocity of the water at the surface is different from that at the depth of the drogue, the drift of the buoy will differ from that of the drogue by an amount depending on the relative drag forces on the buoy, drogue and cable. From their dimensions, and assuming appropriate drag coefficients for the drogue, buoy and cable, the following correction formula was derived:

$$V_D = v_D - \alpha(V_S - v_D),$$

where V_S = velocity measured by surface drogue (depth 5 fm), v_D = velocity measured by drogue at depth D, V_D = corrected velocity at depth D and α is a

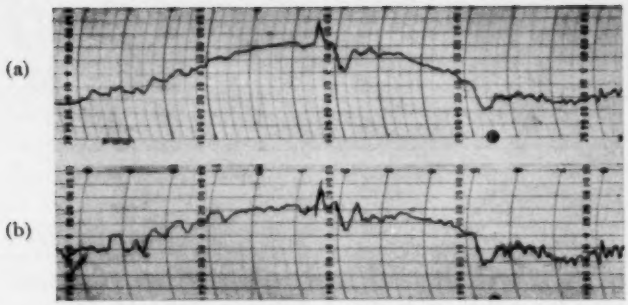

FIG. 5.—Corresponding disturbances on the two cables, 1957 April 26 20 00 h to 1957 April 27 08 00 h. (a) Portpatrick, (b) Nevin.

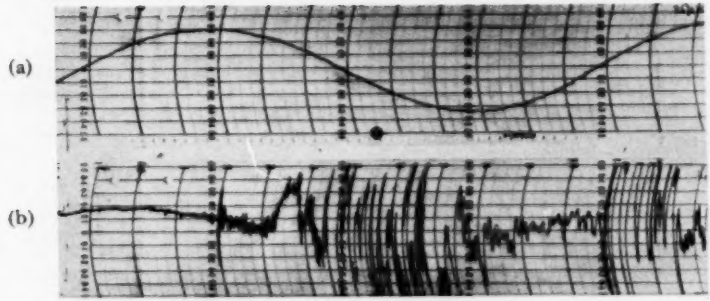

FIG. 6.—Comparison of two Portpatrick records to show: (a) a calm period with no interference due to fluctuations of the Earth's magnetic field. (b) the effect of a magnetic storm.

[Facing page 270

(a)

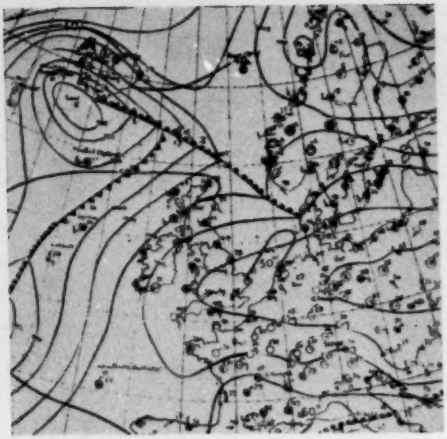

(b)

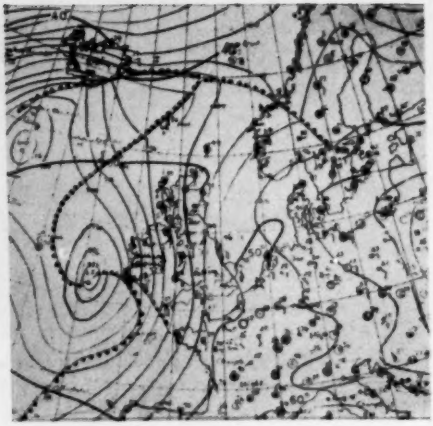

(c)

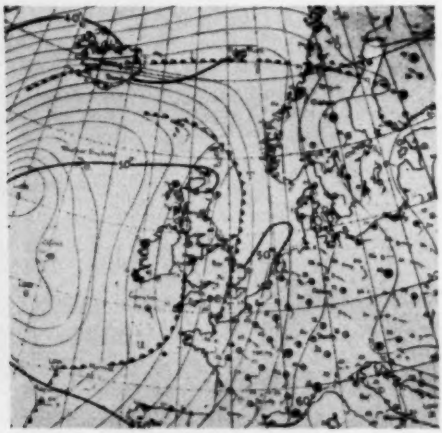

FIG. 11.—Weather situation at 06 00 h on (a) 1955 November 1, (b) 1955 November 2, (c) 1955 November 3. (Crown copyright; reproduced from the Daily Weather Reports issued by the Meteorological Office by permission of the Controller of H.M. Stationery Office).

coefficient, having the value 0·3 for a drogue at 25 fm, 0·34 at 50 fm and 0·4 at 100 fm.

The buoys with drogues set at three depths were released close together, at a position fixed by taking bearings on landmarks with a sextant. The position of each buoy was determined subsequently, at intervals of ½ to 1 hour, by bringing the boat near to it and taking bearings in the same way. As long as the buoys remained in the general area of the station and within reasonable steaming distance of one another, they were allowed to drift freely. When they had drifted too far apart, usually after several hours, or had moved too far from the nominal position of the station, they were taken out of the water and released together again at the starting point. The main limitation of the method was that set by visibility and hours to daylight, since the *William Herdman* was not fitted with any radio navigational aid and all positions were fixed by visual observations.

The positions of the stations and the periods of observation are shown in Table 1. Owing to the limitations referred to above, it was not possible to obtain observations over a complete tidal period in each position. However, at each of the three stations on the successive days 1956 July 9, 10 and 11, observations were made over the full duration of the ebb flow, and these three sets of data were combined to provide an estimate of the total flow across the section during the ebb. At the central station, No. 2, on July 25, the observations extended over 9 hours and included both the maximum flood and maximum ebb currents.

Table 1

Calibration of North Channel cable. Positions and periods of drogues observations

Station, depth, approx. position	Mean position		Date July	Period of observations hours	Hours relative to *HW*
	Lat. N	Long W			
1. 98 m 5 ml. NE of Donaghadee	54° 42′·0	5° 24′·7	9	6	*HW* + ½ to *HW* + 6½
2. 240 m 7 ml. SW of Portpatrick	54° 45′·6	5° 15′·6	10	8	*HW* − 2 to *HW* + 6
3. 130 m 4 ml. SW of Portpatrick	54° 47′·6	5° 12′·8	11	8	*HW* − 2 to *HW* + 6
2. 240 m 7 ml. SW of Portpatrick	54° 45′·6	5° 15′·6	25	9	*HW* − 4½ to *HW* + 4½

By plotting the successive positions of the drogues, the components of drift velocity were determined and corrected for the drag of the buoy and wire, as described above. The corrected velocity component along the channel, taken as positive in direction 150° true, will be denoted by U. The values of U at each depth, at a given station, were plotted as a function of time and the values at hourly

intervals relative to *HW* were read off. Since the three drogues were near the surface, approximately at mid-depth and near the bottom respectively, a simple arithmetic average was taken as the depth-mean $\bar{U}$ of the velocity component at each hour. The mean velocity perpendicular to a section across the whole channel was then taken as

$$\bar{U} = \tfrac{1}{4}(\bar{U}_1 + 2\bar{U}_2 + \bar{U}_3)$$

where $\bar{U}_1$, $\bar{U}_2$, $\bar{U}_3$ denote the depth-means at stations 1, 2 and 3, the value at station 2 being given double weight because of the greater depth of water there. Observations taken on the consecutive days, July 9, 10 and 11, when the range of tide at Belfast was 9·5 ft, 9·4 ft, and 9·3 ft respectively, were combined for this purpose.

At the central station, No. 2, the amplitudes of the velocity components, U_9, $U_{91.5}$ and U_{183}, at the three depths are shown in Table 2. The Table shows also the velocity ratios and the time interval by which the current maximum at 91·5 and 183 m occurs earlier than at 9 m.

Table 2

Calibration of North Channel cable: Velocities at central station.

Date	U_9 cm/s	$U_{91.5}$ cm/s	U_{183} cm/s	$\frac{U_{91.5}}{U_9}$	$\frac{U_{183}}{U_9}$	Time difference $U_{91.5}-U_9$ min	Time difference $U_{183}-U_9$ min
10 July	165	144	126	0·87	0·77	18	21
25 July	107	104	95	0·97	0·89	6	33
Mean	—	—	—	0·92	0·83	12	27

At station 3, mean depth 130 m, it was found that $U_{46}/U_9 = 0{\cdot}86$, $U_{91.5}/U_9 = 0{\cdot}75$, while the phase differences were 7 min and 20 min respectively.

Considering the variation in depth-mean velocity across the section,

$$\bar{U}_1/\bar{U} = 0{\cdot}94,\ \bar{U}_2/\bar{U} = 1{\cdot}05,\ \bar{U}_3/\bar{U} = 0{\cdot}97$$

in the above notation. The phase of the current was 15 min earlier at station 1, and 3 min later at station 3, compared with station 2.

The mean current across the section, $\bar{U}$, was compared with the mean cable voltage $\bar{V}$, as a function of time relative to *HW* for the same period, July 9, 10 and 11, as the drift observations. Before this could be done, however, the calibration of the recording milliammeter in terms of the voltage across the cable was required, and this was done simply by introducing a known e.m.f. into the circuit containing the cable resistance and the recorder. The calibration factor derived in this way was

$$1 \text{ volt} = 149 \text{ cm/s } (2{\cdot}90 \text{ kt}).$$

For July 25, drift observations were available for the central station only, but mean values for the whole section were inferred, assuming the same ratio as found during the previous period. The calibration factor thus deduced was

$$1 \text{ volt} = 122 \text{ cm/s } (2{\cdot}37 \text{ kt}).$$

Taking the average of these two calibration factors, the mean calibration factor is

$$1 \text{ volt} = 135 \text{ cm/s } (2{\cdot}62 \text{ kt}).$$

This value may be compared with that found from the *Cook* measurements. From the drogue measurements, the mean current across the section was 0·87 times the current at 5 fm (9 m) in the centre of the channel. Applying this factor to the *Cook* observations

$$1 \text{ volt} = 0{\cdot}87 \times 167 \text{ cm/s} = 145 \text{ cm/s } (2{\cdot}81 \text{ kt})$$

which is in fair agreement with the drogue measurements.

The calibration factor for the St. Margaret's Bay to Sangatte cable was shown to vary from time to time and as might be expected it fluctuated with the seasonal variation of the electrical conductivity of the sea water. For the Straits of Dover the variation of the calibration factor was investigated in the following way: if R_V = range of velocity, R_E = range of voltage and R_H = range of elevation which was obtained from the tidal predictions for Dover, then

$$f = \frac{R_V}{R_H}\frac{R_H}{R_E}$$

Having determined R_V/R_H it was then assumed constant, and R_H/R_E was examined to determine changes of f. In the case of the North Channel cable the same method was adopted, but R_H was found from the tidal levels at Belfast, the nearest standard port. Unlike Dover, however, Belfast is not directly on the coast, but is at the head of a shallow lough, and as a result the tidal range there does not seem to bear a constant relation to the range of currents in the North Channel. This is further confirmed by the fact that the harmonic constants for the Belfast tidal elevations differ from those of the North Channel currents. For this reason the results obtained were not consistent and it was decided to use the calibration factor derived in 1956 July for all the analysis. The change in calibration expected, due to the change in κ_0/κ_1, is about 10 per cent, which is no greater than the errors involved in the direct calibration.

Calibration of the Nevin–Howth cable records. No current measurements were made during the period of cable signal recording so that the calibration is indirect and relies on data tabulated in Tidal Streams, Part II, together with other indications of spring rates on Admiralty charts. These estimates are for surface flows and were multiplied by 0·87 to give the depth mean velocities. The mean current range across the whole section obtained from these values was compared with the cable voltage range, averaged over springs for six months, to give a calibration factor f, of 1 volt = 106·2 cm/s.

5. Effective electrical conductivity of the sea bed

If the sea bed were perfectly insulating, the potential difference across the channel would be equal to the e.m.f. E given by

$$E = VH_zL \times 10^{-8} \text{ V}$$

where V = mean velocity across the section, H_z = vertical component of the Earth's magnetic field and L = width of channel. The ratio $\delta = e/E$ may then

be determined where e is the observed P.D. across the cable. If the sea bed were a perfect conductor the cable signal would be effectively short circuited and then $\delta = 0$, as $e = 0$. On the other hand if no return current could pass through the sea bed then $\delta = 1$, and $e = E$. Values of δ for the Irish Sea cables are given in Table 3 and show that the shunting effect of the sea bed has reduced the signal E by about a half.

If the cross-section of the channel is represented approximately by a semi-ellipse of major axis L and semi-minor axis D, and if κ_0, κ_1 are the specific conductivities of the sea bed and the sea water respectively, then, as shown by Longuet-Higgins (1949)

$$\frac{\kappa_0}{\kappa_1} = \frac{2D}{L}\left(\frac{1}{\delta} - 1\right).$$

Values of κ_1 were determined for each area from observations of the temperature and salinity of the sea water, and enabled the estimates of κ_0, given in Table 3 to be made.

It will be noticed that although the effective conductivity of the sea bed below St. George's Channel ($8{\cdot}51 \times 10^{-5}$ [ohm. cm]$^{-1}$) is similar to that below the southern North Sea ($13{\cdot}39 \times 10^{-5}$) and the Straits of Dover ($9{\cdot}74 \times 10^{-5}$), the effective conductivity of the sea bed below the North Channel is approximately three times that in the other areas.

6. Methods of analysis of the records

(a) *General*

The deflection of the recorder traces from the zero line was read off at hourly intervals and converted, by a calibration factor determined as in Section 4, to the mean water current across the section. By multiplying the current by the cross-sectional area, the rate of transport of volume of water through the section was found. The long period mean of these values was used as a zero reference in the graphical representation of the results. It must be emphasized, however, that this is not intended to imply that the drift current was zero when averaged over a long period, but is merely a convenient method of representing the variations of the flow.

(b) *Tidal currents*

(i) A harmonic analysis was used on a 29 day period of observations on the Portpatrick to Donaghadee cable record. The method employed is detailed in the Admiralty Tide Tables, Part III (Doodson & Warburg).

(ii) Periodogram analysis was used on three records of hourly readings over 29 days. The computations were carried out on a digital computer (DEUCE) and for the 696 hourly observations of each series 348 periods between 2 and 696 hours were tested. The termination of the programme at a trial period of 2 hours is a consequence of the observations being taken at hourly intervals, and shorter periods could be tested by taking readings at closer intervals. For tidal purposes, however, the two hour limit is adequate. With only 696 observations in the time series, the resolution of the periodogram is particularly poor in the region of the diurnal period, where adjacent test periods are separated by about 50 min. As the higher frequencies are tested, however, the resolution improves so that at 2 hours

Table 3

Effective electrical conductivity of the sea bed

Location	Cross-sectional area (km^2)	Effective cable length (perp. to current) (km)	Mean depth (m)	H_z G	$\delta = e/E$	Equivalent semi-ellipse L(km)	Equivalent semi-ellipse D(m)	$10^3 \kappa_0/\kappa_1$	$10^3\kappa_1$ $(ohm\ cm)^{-1}$	$10^5\kappa_0$ $(ohm\ cm)^{-1}$
N. Channel, Irish Sea (Portpatrick–Donaghadee cable)	4·04	34·6	116·7	0·452	0·475	34·6	138·4	8·84	38·7	34·21
St George's Channel, Irish Sea (Nevin–Howth cable)	7·59	104·2	72·8	0·446	0·432	104·2	84·0	2·14	39·8	8·51
Straits of Dover (St Margaret's Bay–Sangatte cable)	1·20	34·2	35·3	0·43	0·535	34·2	44·9	2·29	42·6	9·74 (3·4)*
Southern North Sea (Aldeburgh–Domberg)	4·44	145·0	30·6	0·43	0·145	145·0	39·0	3·20	41·8	13·39 (7·2)*

* Longuet-Higgins (1949), based on only a short period of observation.

the separation is only 0·3 min. This means that higher harmonics are easily distinguishable from the background and there is little interference between the constituents.

(c) *Residual currents*

For most of the analysis the main tidal influence was eliminated from the record, and an estimate of the daily residual drift was obtained by taking the average of 25 consecutive hourly values of the current centred at noon.

Where a detailed analysis for a selected period was required when a high rate of flow was observed for a short time, the above method was inadequate and the hourly residual current was determined by storm surge analysis (Rossiter 1959).

(d) *Subsidiary data*

One of the main objects of the investigation was to examine the relationship between the variations of the flow of water through the North Channel and the variations of the sea surface wind. The daily mean winds were required therefore and were obtained from the Meteorological Office Daily Weather Reports, where wind velocities are given for numerous stations at 6 hourly intervals. For some time observations of the wind at West Freugh, a position fairly close to the North Channel, were used. Later on, however, measurements at certain times were discontinued, and it was decided to use wind data from another source.

An attempt was then made to compute the sea surface wind from atmospheric pressure observations at Malin, Renfrew and Valley. The results obtained, however, were higher than any observed winds and it was concluded that the method was unsuitable in the present application, partly because of the nearness of the stations and partly because of unsteady atmospheric conditions. As an alternative the daily means of the winds recorded every six hours at Ronaldsway and Prestwick were adopted for the analysis, it being considered that these would represent the winds over the northern Irish Sea and the approaches to the North Channel.

The storm surge analysis of the cable record for the period between 1955 October 31 and 1955 November 6 required more detailed wind data and this was kindly supplied by the Meteorological Office of the Air Ministry in the form of hourly recorded winds at West Freugh.

7. Results

(a) *Tidal analyses and periodograms for selected periods*

A harmonic analysis was carried out on a 29 day period of observations of the Portpatrick–Donaghadee cable signal between 1955 July 12 and 1955 August 9, when the winds over the Irish Sea were fairly light. The method employed is detailed in the Admiralty Tide Tables, Part III, and the results in terms of amplitudes in cm/s and phases in degrees of the tidal constituents M_2, S_2, N_2, K_1, O_1, P_1, M_4, MS_4 are given in Table 4. It will be noticed that a large proportion of the tide was due to the lunar semidiurnal constituent M_2, which was nearly three times larger than its nearest rival.

Although the above analysis indicates the contributions from the major tidal constituents it gives no indication of other oscillations present, whether tidal or otherwise, and it was decided, therefore, to carry out a periodogram analysis on the same data. The resulting periodogram is shown in Figure 7(a). The pre-

Table 4

Harmonic constants of North Channel cable record

(Amplitudes in cm/s: phases in degrees)

	M_2	S_2	N_2	K_1	O_1	S_1	M_4	MS_4
Harmonic analysis: Amplitude	77·7	28·2	17·6	0·8	1·2	—	2·0	1·4
Phase	42	81	13	205	155	—	339	354
Periodogram: Portpatrick, 1955 July 12–August 9: Amp.	77·4	27·4	17·7	1·0	1·2	1·4	2·0	1·4
Amplitude ratio	1·00	1·03	0·99	0·80	1·00	—	1·00	1·00
Periodogram: Portpatrick, 1957 July 16–August 13: Amp.	87·7	31·4	14·8	0·5	1·5	2·1	1·9	0·8
Periodogram: Nevin 1957 July 16–August 13: Amp.	86·9	24·1	11·5	1·4	0·9	6·9	4·0	2·0

dominance of semidiurnal oscillations is immediately obvious as a series of high peaks in the region of 12 hours. Diurnal harmonics were also present although interference between the individual diurnal constituents was inevitable, due to the low resolving power of the periodogram in that part of the spectrum. This poor resolution could be improved considerably by taking one year's observations instead of 29 days. A number of other peaks are in evidence and all of them could be accounted for in terms of oscillations of tidal origin. Tidal currents are often richer in the higher harmonics than tidal elevations, so it was not surprising to find that a number of these oscillations, with periods at or near 3, 4, 6 and 8 hours, were definitely present in relatively large amplitudes.

The amount of energy associated with the periods present may be estimated from the periodogram by a process described by Davis (1941). When applied to the peaks of the semidiurnal tide this method revealed that about 98 per cent of the energy of the time series was contained in the harmonic constituents M_2, S_2 and N_2.

To compare the constituent amplitudes given by the harmonic analysis and the periodogram analysis, the amplitude of test periods in the periodogram nearest to the appropriate tidal period were noted and are given in Table 4. The amplitude ratio shows the closeness of the two sets of estimates. The diurnal constituents may be somewhat different from those of the true water movement because the cable also detects Earth currents which are known to have oscillations of diurnal period.

The method of periodogram analysis using a digital computer is speedy and extensions to the reduction of tidal data in general seem promising.* However, the purpose of the present work was to examine the periodicities of the time series to decide if there were any periods present which were not of tidal significance. In fact all the significant periods appeared to be related to tidal oscillations.

The same analysis was also applied to hourly observations taken at Portpatrick and Nevin during the 29 day period between 1957 July 16 and August 13. The results in periodogram form are shown in Figure 7(b) and 7(c), and the amplitudes corresponding to common tidal harmonic constituents are given in Table 4. In the case of the Portpatrick series the significant periods are present in similar proportions, so that there were no obviously transient periods in the records. The Nevin periodogram shows that the higher tidal harmonics were again present, although the diurnal constituents of the tidal currents were more important than in the North Channel.

(b) *Daily values of current*

The 25 h mean values of current in cm/s in the North Channel of the Irish Sea, referred to the long period mean as a zero reference, are shown in Figure 8(a) and (b), where the period of observation extends from 1955 October to 1958 March. Similar values of the mean velocity across the Nevin to Howth section (St. George's Channel) are shown (Figure 8(b)), although these measurements were only carried out from 1957 January 1 to 1958 March 31. The vertical scale is also graduated in units of time rate of transport of water, viz. km^3/day, thus taking into account the cross-sectional area over which the currents operate. For example, with the same mean current of 10 cm/s for the whole cross-section the transport across the Nevin–Howth section (effective area 6·879 km^2) would be 59·5 km^3/day,

* Mr. D. E. Cartwright of the National Institute of Oceanography has developed the method to analyse tidal data in the English Channel.

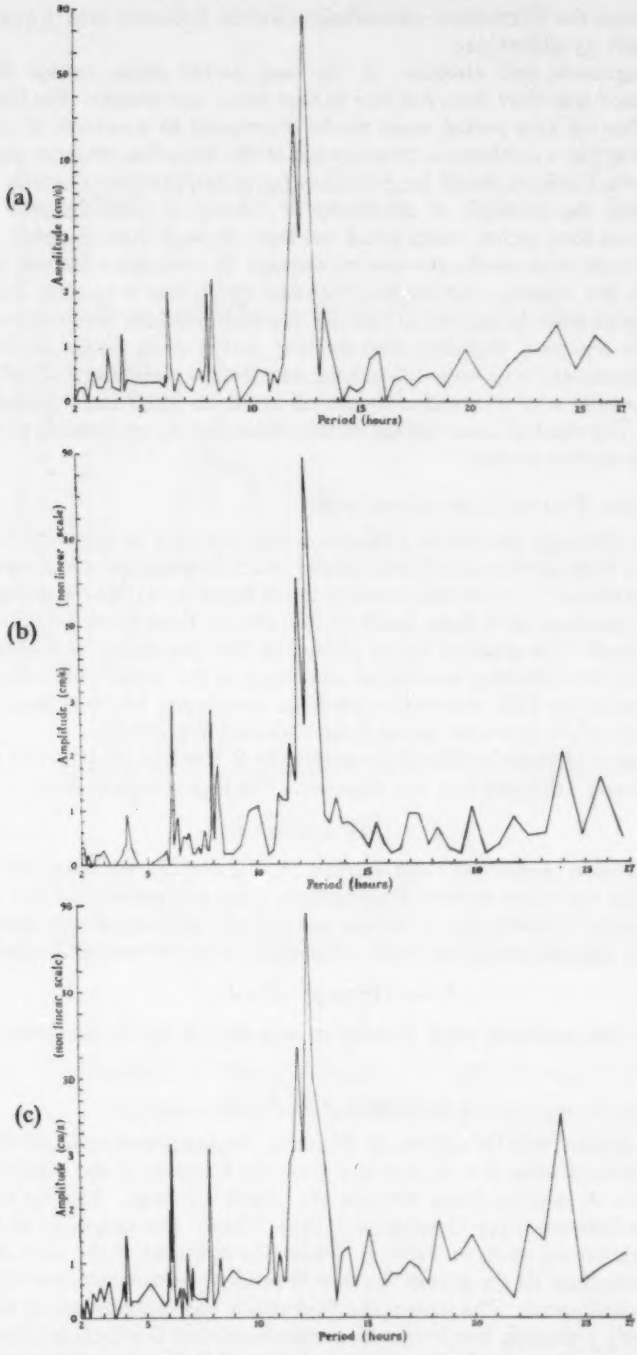

FIG. 7.—Periodograms derived from hourly observations extending over 29 days. (a) Portpatrick, 1955 July 12 to 1955 August 9. (b) Portpatrick, 1957 July 16 to 1957 August 13. (c) Nevin, 1957 July 16 to 1957 August 13.

whereas across the Portpatrick–Donaghadee section (effective area 3·933 km²) it would be only 33·98 km³/day.

The magnitude and direction of the long period mean voltage for each cable indicated that they were not due to true water movements. For the North Channel cable the long period mean would correspond to a current of 2·99 cm/s (10·16 km³/day) in a northwards direction out of the Irish Sea, whereas across the Nevin–Howth Cable it would be 7·30 cm/s (43·41 km³/day) southwards. These results violate the principle of continuity of volume of water because on the average, over a long period, water could not leave through both channels. Moreover, the annual mean northward current through St. George's Channel, as determined from the velocity distribution (Bowden 1950), was 0·35 cm/s, which, as well as being an order of magnitude less than the cable estimate, was in the opposite direction. It was clear, therefore, that the long period mean voltage on the cable could not represent a true water movement, and that no profitable study of the net water movements over a considerable period could be made from the cable observations. The residual mean voltage on the cables may be attributable to features of the Earth current system.

(c) *Correlation of current with regional winds*

The flow through the North Channel is due not only to the local frictional effects of the wind on the sea surface but also to the longitudinal surface gradients which are produced by wind effects over a much larger area. No computations of sea surface gradients have been made in this area as there were no tide gauges suitably located. The gradient forces producing flow are mainly secondary wind effects and in the following correlation analysis it is the mean wind over a considerable area of the Irish Sea and its northern approaches which is used, so that the effects of surface gradients are taken into account implicitly.

The method of analysis follows the procedure of Bowden (1956) when a linear relation between wind and flow was assumed. The regression equation

$$V = cW_N + dW_E + I \qquad (1)$$

has two regression coefficients c and d, while V, W_N and W_E are the mean velocity in cm/s across the whole section, the northerly wind component and the easterly wind component respectively. The last term, I, is that part of the flow which appears to be independent of the wind. Equation (1) may be written in the form

$$V = AW\cos(\theta - \alpha) + I \qquad (2)$$

where W is the resultant wind velocity in m/s and A and α are given by the conditions:

$$c = A\cos\alpha, \quad d = A\sin\alpha.$$

From (2) it appears that for a given A, W and α, the maximum value of the mean flow V is obtained when $\theta = \alpha$, that is α gives the direction of the wind which is most effective in moving water through the North Channel. For the series of observations between 1955 October and 1958 March, the constants of the regression equation are given in Table 5. Under the influence of the most effective wind (i.e. from S 49° E) the part of the flow dependent on the wind was 0·956 per cent of the wind speed. The part of the flow which was independent of the wind was apparently 3·36 cm/s, but it must be remembered that this included the effects of earth currents on the cable, and as a result it is of little value. The compound

correlation coefficient $R_{1(23)}$ gives a measure of the goodness of fit between the mean flow and a linear combination of the wind components, and its value in this case was fairly high and equal to 0·68. Without doubt there was a significant relation between the wind and the water movement.

Initially it was suspected that there was some inequality in the magnitude of the effects of opposite winds. More specifically it looked at first sight as if a northerly flow was produced more readily than a southerly one. This might, on the one hand, have been due to unequal exposure to all directions at the wind measuring stations, or on the other hand, to the effect of the different physical characteristics of the northern and southern approach areas of the North Channel.

To resolve this difficulty the observations were sorted into two groups, in one of which the daily mean wind had a component towards N 27°W along the axis of the channel, and in the other it had a component in the opposite direction towards S 27°E. The summer and winter periods were considered separately and the computed regression equations are shown in Table 5. Although there is a difference between seasonal values the two groups are similar, and it was concluded that all observations could be given equal weight.

The question of seasonal variations of correlation also presents itself and to investigate this possibility, in the first instance, winter (October–November) and summer (April–September) observations were considered separately. The constants of the regression equations are given in Table 5, and it will be noted that the total correlation coefficient $R_{1(23)}$ for the winter series was a good deal higher at 0·77 than for the summer series when it was 0·42. Similarly, the value of A was somewhat higher at 1·152 in winter than in the summer when it was 0·767.

As a result the data were further analysed in bi-monthly periods so that the correlation variations could be studied in more detail. The computed coefficients are given in Table 6, which includes the results of computations from records taken between 1954 December and 1955 September, although they have not been included in the main analysis. When studying these results it was suspected that the recorder biassing arrangements were unsatisfactory and consequently a centre zero instrument was fitted in 1955 October to replace the original side zero recorder. The immediate effect was to reduce the value of I considerably. The changes of the bi-monthly root mean square wind $(\overline{W^2})^{\frac{1}{2}}$ and $R_{1(23)}$ with the seasons are also shown. In Figure 9 $R_{1(23)}$ is plotted against $(\overline{W^2})^{\frac{1}{2}}$ the root mean square wind speed, showing that $R_{1(23)}$ tends to increase with $(\overline{W^2})^{\frac{1}{2}}$. The seasonal change in $R_{1(23)}$ is therefore related to the fact that higher wind speeds were experienced in the winter than in the summer.

The values of A shown in Table 6 vary from one bi-monthly period to another with extreme values of 0·522 and 1·567 during the main series of observations. It was apparent that a high correlation existed between A and $(\overline{W^2})^{\frac{1}{2}}$ and this is illustrated in Figure 10. A linear regression formula computed under the least squares criterion to fit the data was

$$A = 0{\cdot}2313(\overline{W^2})^{\frac{1}{2}} - 0{\cdot}386. \quad 4 < (\overline{W^2})^{\frac{1}{2}} < 8.$$

The results seem to indicate that it would have been better to correlate the mean flow with the square of the wind velocity, to secure a less variable value of A. Nevertheless, the method adopted still provides a post prediction flow formula where only the wind velocity is utilized, although it should be pointed out that the

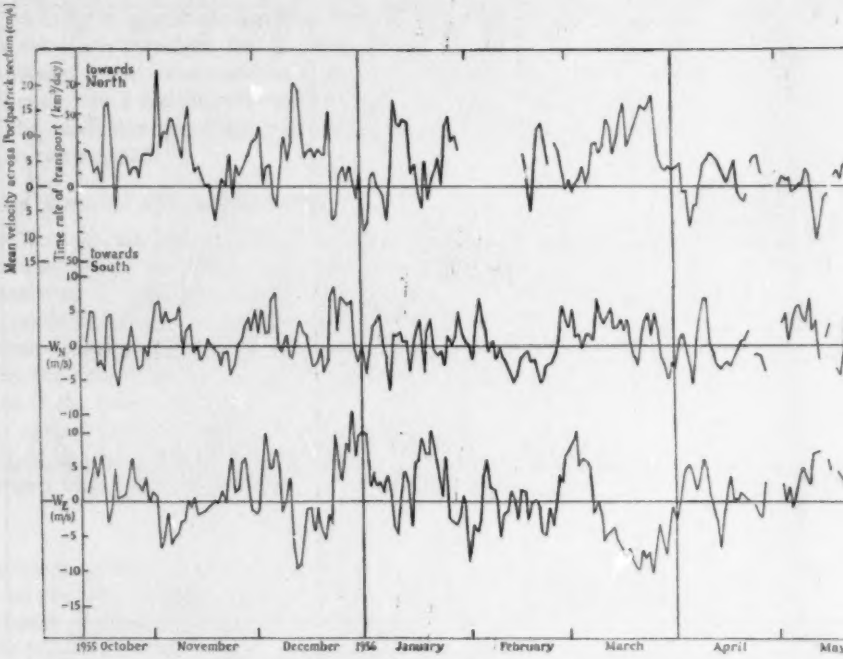

FIG. 8(a).—Daily mean values of current through the North Channel ar

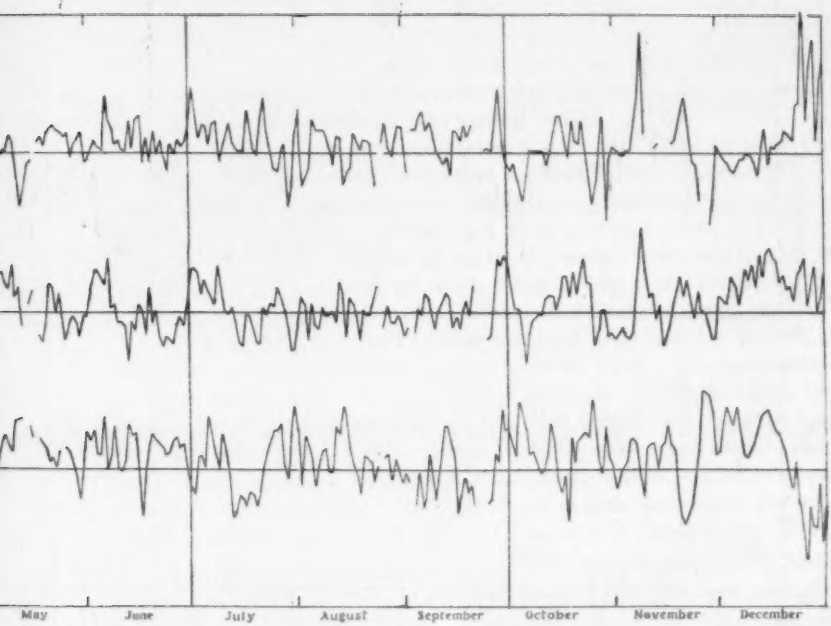

el and the wind components. 1955 October 11 to 1956 December 31.

[*Facing page 280*

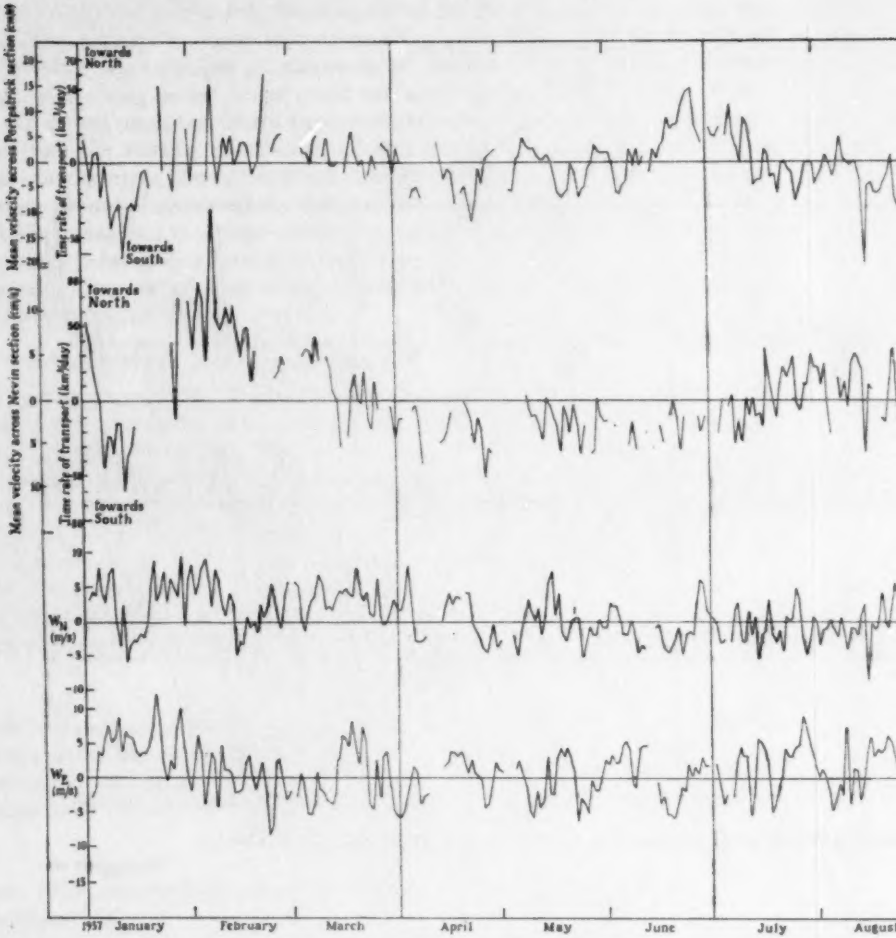

FIG. 8(b).—Daily mean values of current through the North Channel and St George

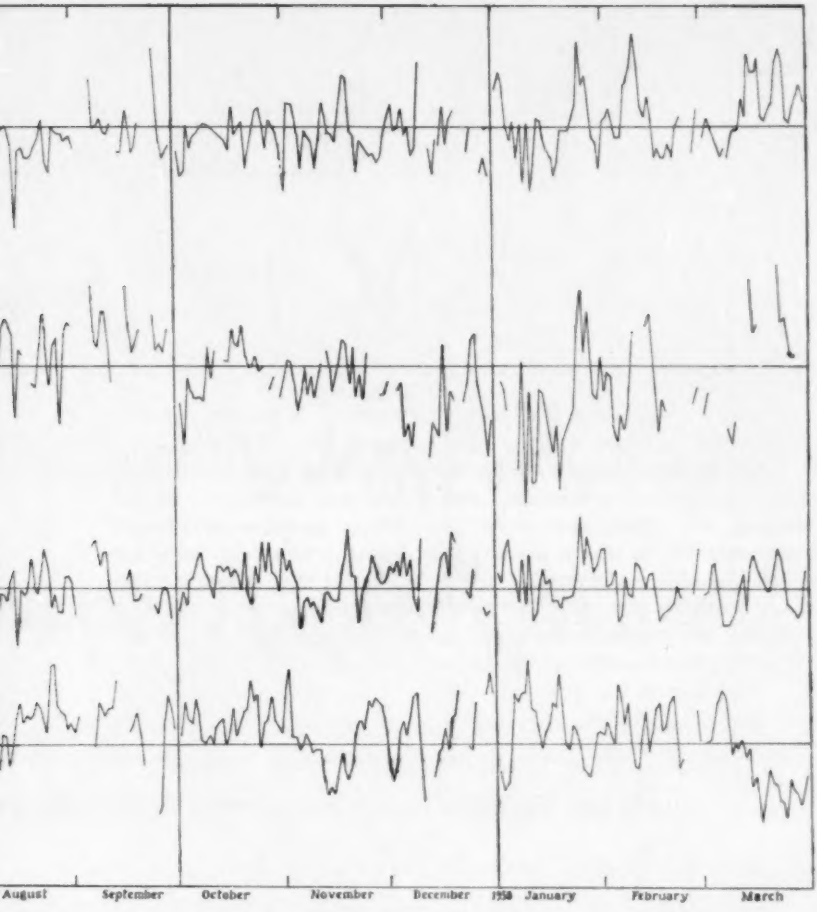

eorge's Channel and the wind components. 1957 January 1 to 1958 March 31.

Table 5

Correlation of Portpatrick–Donaghadee cable records and mean winds in 6 monthly periods, and comparable results for the Straits of Dover

Locality	Period	Mean wind has components towards	A	α°	I	No. of Obs.	$R_{1(23)}$	s.e. of A
North Channel of Irish Sea	Winter 1955/56, 1956/57, 1957/58, October–March	N 27° W	1·213	49	4·15	268	0·73	0·072
	Winter 1955/56, 1956/57, 1957/58, October–March	S 27° E	1·043	44	3·40	220	0·51	0·106
	Winter 1955/56, 1956/57, 1957/58, October–March	All obs.	1·152	47	3·31	488	0·77	0·039
North Channel of Irish Sea	Summer, 1956, 1957 April–September	N 27° W	0·617	59	3·08	133	0·44	0·120
	Summer 1956, 1957 April–September	S 27° E	0·833	39	3·51	198	0·58	0·095
	Summer 1956, 1957 April–September	All obs.	0·767	52	2·91	331	0·42	0·064
North Channel of Irish Sea	1955 October–1958 March	All obs.	0·956	49	3·36	819	0·68	0·034
Straits of Dover	1953 March 1–August 31 (Summer)		2·25	39			0·77	0·35
	1954 September 1–March 31 (Winter)		3·6	16			0·83	0·35

linear formula tends to overestimate the low flows and underestimate the high ones (See also Section 7(d)).

The values of the coefficient A for the North Channel, in both the summer and winter periods, are approximately one third of those for the Straits of Dover.

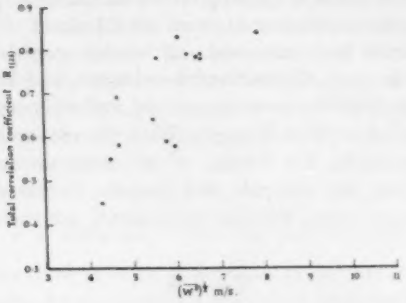

FIG. 9.—Variation of the total correlation coefficient, $R_{1(23)}$ with the root mean square wind speed, $(\overline{W^2})^{\frac{1}{2}}$.

This is probably due to the fact that the North Channel section is 3·3 times as deep as that in the Straits of Dover and has a less constricting effect on the flow. The ratio of the cross-sectional areas of the Nevin–Howth and North Channel sections, from the values in Table 3, is 1·88. In the English Channel, on the other hand, the ratio of the cross-sectional area of a section from Portland Bill to Cap de la Hague to that of the section in the Straits of Dover is 4·56.

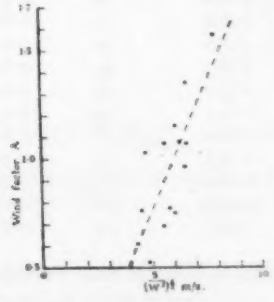

FIG. 10.—The wind factor, A, as a function of the root mean square wind speed, $(\overline{W^2})^{\frac{1}{2}}$.

(d) *Results of detailed analysis for a selected period*

Heavy gales were experienced over the Irish Sea on 1955 November 2, and the effect on the cable signal was easily detected as a displacement of the whole trace from its usual mean position. This section describes the detailed analysis of the record for the period from October 31 to November 6. The general meteorological situation, before and during the period of the storm surge, is interesting, and it will now be described briefly before proceeding to the analysis and the results.

The sequence of events can be followed on the Meteorological Office weather charts which are reproduced in Figure 11 for 0600 on November 1, 2 and 3. Although an anticyclone persisted for a few days over the eastern Atlantic before October 31 it then moved eastwards across England and a depression off Iceland drifted slowly south. On the next day a complex low to the west of the British Isles moved south, with some deepening, and was followed by another deepening depression which moved south-east from off west Iceland. The wind, which had been light over the Irish Sea, increased and became southerly. During the early part of November 2 the deep depression moved north, and later on the winds over the northern part of the Irish Sea were very strong and at times gusts of over 28·3 m/s (55 knots) were recorded at West Freugh. With the movement of the low northwards and then westwards, the winds, which were south and south-easterly, moderated, and by next day the gale had abated. It was during November 2, when the winds were so strong, that the cable signal was mainly affected.

Table 6

Correlation of cable records and mean winds in bi-monthly periods

Period	A	$\alpha°$	$R_{1(23)}$	I	$(\overline{W^2})^{\frac{1}{2}}$ m/s
•1954 Dec–1955 Jan	1·36	70	0·79	14·32	7·8
•1955 Feb–Mar	1·46	39	0·83	21·72	5·7
• Apr–May	0·35	13	0·36	15·54	5·4
• June–July	0·28	119	0·33	13·83	4·3
• Aug–Sept	0·47	94	0·39	17·10	4·8
Oct–Nov	1·028	21	0·69	4·85	4·7
Dec–1956 Jan	1·351	61	0·78	6·32	6·6
1956 Feb–Mar	0·963	47	0·78	4·90	6·5
Apr–May	0·704	77	0·58	2·81	4·7
June–July	0·688	39	0·64	2·83	5·5
Aug–Sept	0·759	43	0·55	2·21	4·5
Oct–Nov	1·151	32	0·83	0·88	6·1
Dec–1957 Jan	1·567	41	0·84	0·01	7·9
1957 Feb–Mar	0·766	48	0·59	3·55	5·8
Apr–May	0·611	44	0·45	0·91	4·3
June–July	0·522	47	0·30	6·08	4·8
Aug–Sept	0·752	49	0·58	3·16	6·0
Oct–Nov	1·074	42	0·78	1·74	5·6
Dec–1958 Jan	1·074	34	0·79	2·15	6·6
1958 Feb–Mar	1·076	33	0·79	5·20	6·3

• Not included in main analysis—see text.

The first step in the analysis was to remove the tidal effects from the cable record, but where features of flow during a day are required, the rather crude method of taking a 25 hour mean is unsuitable. A method of analysis was designed by Rossiter (1959) to extract storm surges from tidal records and is applicable to the present work. The diurnal, semi-diurnal and quarter-diurnal tides are estimated and removed, to leave hourly residuals, from which a large proportion of the effect of the tide is eliminated. The results for the period from 1955 October 31 to 1955 November 6 are tabulated and the mean current pulse which occurred during November 2 is shown in Figure 12. For the most part the magnitude of the residuals was small except during the central day, when a considerable non-tidal

flow of about 41 cm/s, averaged over the whole cross-section of the channel, was present. There was also a secondary peak on November 4, which was again closely associated with the wind.

Having obtained the residuals the method of analysis was similar to that described in Section 7(c). Results of the correlation analyses of the transport and wind over a long period have revealed, that where a linear relation between these two quantities is assumed, the total correlation coefficient varies with the wind speed (see Figure 9), and it is reasonable therefore to correlate the transport indicated on the cable with the square of the wind. In these circumstances the three variables concerned are: (1) the cable transport, (2) $W.W_N$, and (3) $W.W_E$ where W, W_N and W_E are respectively the wind speed, the northerly component of the wind and the easterly component of the wind.

The computed regression equation was:

$$V = 0{\cdot}0922W^2\cos(\theta + 20^\circ 30') + 2{\cdot}058$$

where the hourly mean wind velocity W was in m/s and the mean velocity V across the section was in cm/s. As in a previous section, it indicates that part of the cable signal was not due to wind-induced flow in the North Channel and may be attributed, to an indeterminate extent, to earth current pick up. The goodness of fit of the above formula is shown in Figure 12.

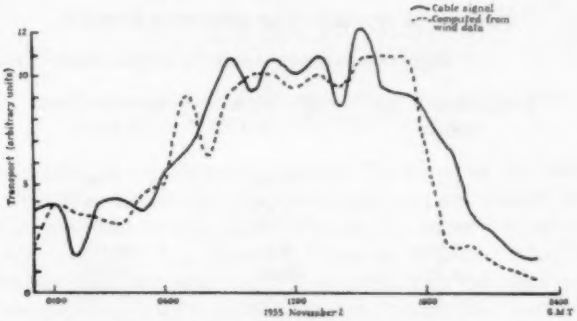

FIG. 12.—Current surge through the North Channel on 1955 November 2. ——— cable signal; - - - - - - - computed from wind data.

It is interesting to examine the primary and secondary correlation coefficients of the foregoing analysis; these are given below:

$$r_{12} = 0{\cdot}827, \quad r_{23} = -0{\cdot}902, \quad r_{13} = -0{\cdot}793.$$

$$r_{12{\cdot}3} = 0{\cdot}427, \quad r_{23{\cdot}1} = -0{\cdot}719, \quad r_{13{\cdot}2} = -0{\cdot}194.$$

The high negative correlation between $W.W_N$ and $W.W_E$ ($r_{23{\cdot}1} = -0{\cdot}719$) shows that for the period of observations, wind components towards the north were associated with components towards the west, that is, there were persistent winds from the south-east quadrant. The low partial coefficient ($r_{13{\cdot}2} = -0{\cdot}194$) showed that correlations of transport and $W.W_E$ were poor so that the apparently high negative correlation given by the primary coefficient ($r_{13} = -0{\cdot}793$) was due mainly to the high correlation of the wind components.

For comparison the bi-monthly period 1955 October–November gave the following correlation coefficients.:

$$r_{12} = 0{\cdot}646, \quad r_{23} = -0{\cdot}361, \quad r_{13} = -0{\cdot}437.$$
$$r_{123} = 0{\cdot}582, \quad r_{23{\cdot}1} = -0{\cdot}115, \quad r_{13{\cdot}2} = -0{\cdot}286.$$

Here the daily mean wind components W_N and W_E, and not $W.W_N$ and $W.W_E$, were correlated with the water transport. The wind was much less persistent ($r_{23{\cdot}1} = -0{\cdot}115$) but, as before, the highest correlation was associated with W_N ($r_{12{\cdot}3} = 0{\cdot}582$). The compound or total correlation coefficient which measures the goodness of fit between the transport and a linear combination of the wind components was 0·69, which is less than for the quadratic formula where it was 0·83.

Referring again to the regression formulae, one would expect a correspondence between the predictions of the formula in terms of the wind velocity and the other in terms of the square of the wind velocity. In Table 7 the computed daily mean flows and the residual movement given by the cable are shown. Whereas in the linear formula the wind velocity is a simple daily mean from six-hourly observations, in the quadratic formula the mean square of the hourly wind velocities, and not the square of the daily mean wind, must be used.

Table 7

Comparison of results from prediction formulae

Date	Daily mean transport velocity across whole of section			
	From storm surge analysis	25hr mean	bi-monthly linear formula	quadratic formula
1955				
Oct 31	4·40	6·02	6·99	2·19
Nov 1	5·04	5·75	10·91	3·45
2	21·37	21·78	13·84	20·43
3	5·97	6·41	10·28	7·24
4	9·37	10·02	10·81	4·80
5	7·19	9·35	10·75	6·75

The tabulated values of the daily residual transport velocities determined by the storm surge analysis and by a simple mean of 25 hourly observations from the cable records, agree reasonably well. The linear regression formula tends to reduce extreme values so that low flows are overestimated, whereas rapid flows are underestimated. In the case of the quadratic formula, however, a better fit is obtained.

During this selected period there was no significant alteration of the daily mean sea level at Liverpool. This was due to the fact that S and SE winds do not appreciably change the sea level at Liverpool, which responds most effectively to a westerly wind acting over the shallow water of Liverpool Bay (Doodson 1924).

(e) *Time dependence of transport generation*

The possibility of the transport lagging the wind effects, although not immediately obvious from the storm surge data, was also investigated. Total correlation coefficients were computed for different lag and lead periods between the square of the wind velocity and the water transport indicated by the cable signal for the same period, 1955 October 31 to November 6. The computations were

carried out on a digital computer (DEUCE) for lead and lag periods of 12 hourly differences on each side of coincidence. These results are shown graphically in Figure 13, and illustrate one rather interesting feature. The highest correlation occurs when the transport is correlated with the wind blowing between one and two hours previously, and the correlation under these circumstances is 0·85. The correlation coefficient differs from that of 0·83 obtained for zero lag by only a small amount, but nevertheless the individual cross correlations seem to indicate

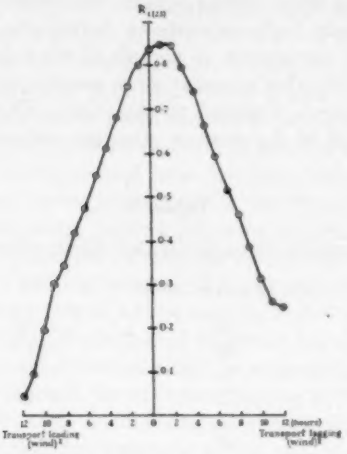

FIG. 13.—Time dependence of the wind produced current between 1951 October 31 and November 6.

that the correlation is significantly increased by allowing the wind to lead the transport. On either side of the maximum value the correlation diminishes with increased time as would be expected. The use of a regression equation associated with a two hour transport lag, does not, of course, improve to any marked degree the fit of the transport computed by this equation with the observed cable signal. It is, however, striking that the water transport through the North Channel reacts so quickly to a wind over the North Irish Sea, the lag being not more than two hours.

(f) *Correlation of Portpatrick–Donaghadee and Nevin–Howth cable records*

The correlation between the recorded daily mean water movements through the North Channel and the St George's Channel were examined for the period from 1957 January to 1958 March. For the whole of that time the correlation coefficient was 0·55 and by Student's t test it is highly significant.

The daily values are shown in Figure 8, where corresponding peaks in the flow across the two sections are easily discerned. There are, however, long period trends associated with the Nevin–Howth record which have no counterpart on the North Channel record. These trends are presumed to represent changes in the cable zero, as they are too large to correspond to actual transports of water. A current of 10 cm/s, for example, flowing for 24 hours across the Nevin–Howth section, with no flow through the North Channel, would produce a change of 2·7 m in the level of the whole of the northern part of the Irish Sea. Such

trends do not occur to the same extent in the North Channel record, although an apparent northward flow in 1957 June and July is probably spurious, as it had no counterpart on the Nevin–Howth record.

To reduce the effects of long period trends, correlation coefficients for 3-monthly periods were computed and are given in Table 8. It will be noticed that in the summer months there was no significant correlation between the flow across the two sections. The winds are, in general, lighter and less persistent at this time of year, and the variations in current, particularly across the Nevin–Howth cable, were evidently not large enough to stand out above the background fluctuations. The comparatively high correlations during the winter months, on the other hand, confirm the occurrence of periods of wind-induced flow through the Irish Sea as a whole. The cable records cannot provide any evidence as to whether the flow from St. George's Channel to the North Channel (or in the reverse direction) is concentrated on the western or eastern side of the Isle of Man.

Table 8

Correlation of Portpatrick–Donaghadee and Nevin–Howth cable records

Date	No. of observations	r	significant
1957 Jan–Mar	66	0·72	yes
Apr–June	60	0·21	no
July–Sept	74	0·27	no
Oct–Dec	75	0·49	yes
1958 Jan–Mar	58	0·78	yes
1957 Jan–1958 June	333	0·55	yes

(g) *Accumulated transport due to wind*

Bi-monthly regression formulae of the form of equation 2, Section 7(b), were given in Table 6 to express the correlation between the wind and the transport of water through the North Channel. One term on the right-hand side of this equation, namely $AW\cos(\theta-\alpha)$, depends on the daily mean wind vector, while the other, I, is not associated with the wind.

An estimate of the daily transport V' due to the wind alone may be made using the relation

$$V' = V - I$$

where V is the daily transport measured on the cable and I is obtained from the regression formula for the particular bi-monthly period.

$$\sum_{n=1}^{n=60} V_n'$$

may then be computed to give the accumulated transport. This has been carried out for six bi-monthly periods between 1956 April 1 and 1957 March 31 and the results are plotted in Figure 14 where the ordinates of the graph are given in (a) km^3 and (b) km per unit area of cross-section. It is revealed that during the year a total of 434 km^3 of water flowed out of the Irish Sea through the North Channel as a result of the action of the wind, which had an annual mean value of 2·2 m/s from the south-west. In terms of a mean flow through the whole section it amounts

to 0·35 cm/s or 0·302 km/day. This current is equivalent to 0·20 cm/s through St. George's Channel over the Nevin to Howth cable, and is of the same order of magnitude, and in the same direction, as the annual mean flow of 0·35 cm/s obtained from a study of the salinity distribution (Bowden 1950).

This suggests that the mean flow deduced from the salinity distribution may be due almost entirely to the residual effect of the wind-induced flow over a long period.

It is also interesting to consider the history of an element of water starting off at any instant in the North Channel. It would drift to the south or north depending on the wind influence, but the time it took to return to the section would vary considerably, depending on the time it started. Figure 13 shows the accumulated movement over one year starting from 1956 April 1, and it will be observed that the maximum displacements to the south and north were 133 km (1956 December 14) and 120 km (1957 March 23) respectively. The interval between adjacent crossings of the section may be determined from the same curve by measuring horizontally along the ordinate corresponding to the day the element left the section, to the time when the curve next reached the same accumulated transport value. This interval would be very short if the element crossed the section just before the transport curve reached a turning point. The interval would be long, however, if the element crossed the section at a time such as 1956 April 2, in which case it would not have returned from its southward excursion for about 273 days.

A long displacement in one direction would be expected to result in the element of water losing its characteristics, by turbulent mixing with other masses, before returning to the North Channel. In this way an irregularly alternating flow could result in a "flushing" of Irish Sea water out of the area, even if no net flow were apparent.

8. Conclusions

The cable method, giving the total flow across a section of the North Channel is complementary to other methods of current determination. It provides a continuous record of the day to day variations in the flow and enables the correlation of the flow with the wind to be established for this area. On the other hand, the cable method does not give any evidence on the variation of flow across the section or on the long-period mean flow. The variation in current across the section can be calculated by Helland–Hansen's method from the distribution of temperature and salinity, but this alone does not enable absolute velocities to be determined. Relative currents have, in fact, been calculated from a number of hydrographic sections across the North Channel, but the results are not discussed in this paper. Neither method is capable of giving a quantitative estimate of the average drift through the North Channel over a long period, and for this one must still refer to the estimate based on the general distribution of salinity and the influx of fresh water into the Irish Sea.

9. Acknowledgments

The authors wish to express their gratitude to the Post Office Engineering Department for the use of the telephone cables. The willing co-operation of the Staffs of the repeater stations who tended the recorders made this investigation possible, and in particular thanks are due to Mr W. Mercer at Portpatrick who gave us the

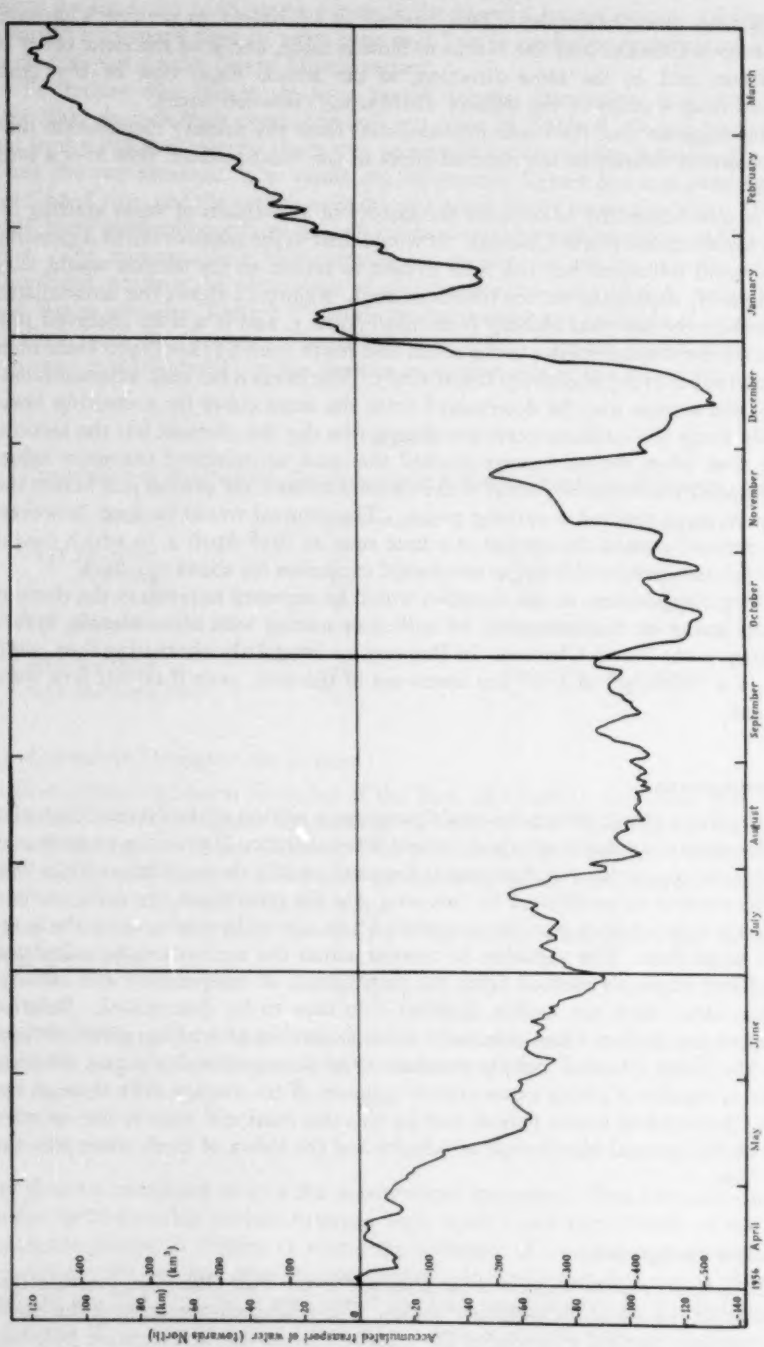

FIG. 14.—Accumulated daily transport of water through the North Channel from 1956 April 1 to 1957 March 31.

utmost assistance. We wish to acknowledge the co-operation of the Hydrographic Department of the Admiralty, in arranging for current measurements to be made by H.M.S. *Cook*, and of the Meteorological Office in providing wind data.

Department of Oceanography,
University of Liverpool.
1961 *January* 3.

References

Admiralty. *Tidal Streams: European Waters.*
Bowden, K. F., 1950. *Mon. Not. R. Astr. Soc. Geophys. Suppl.*, **6**, 63.
Bowden, K. F., 1956. *Phil. Trans. Roy. Soc. A.*, **248**, 517.
Daniel, R. J. and Lewis, H. M., 1929. *Lancs. Sea-Fish. Lab. Reports*, **38**, 36.
Davis, H. T., 1941. *The Analysis of Economic Time Series.* Principia Press, Cowles Commission for Res. in Economics, Mon. No. 6.
Knudsen, M., 1907. *Cons. Int. Explor. Mer.*, Publ. de Circ. No. 39.
Longuet-Higgins, M. S., 1949. *Mon. Not. R. Astr. Soc. Geophys. Suppl.*, **5**, 285.
Proudman, J., 1939. *Mon. Not. R. Astr. Soc. Geophys. Suppl.*, **4**, 387.
Rossiter, J. R., 1959. *Dtsch. Hydrog. Z.*, **12**, 117.
Tait, J. B., 1952. *Cons. Int. Explor. Mer., Ann. Biol.* **8**, 94.
Williamson, D. I., 1956. *J. Mar. Biol. Assoc. U.K.*, **35**, 461.

Upper Mantle Structure under Oceans and Continents from Rayleigh Waves*

Keiti Aki† and Frank Press

(Received 1961 February 7)

Summary

Theoretical seismograms of Rayleigh waves based on several models of mantle structure are compared with actual records for various paths. It is found that the model 8099 of Dorman, Ewing and Oliver explains seismograms for Pacific paths but does not agree with records from Indian–Atlantic ocean paths in the period range shorter than about 100s. The velocity of the Airy phase corresponding to the group velocity maximum is about 0·10 km/s lower for the Indian–Atlantic path than for the Pacific. This difference can be accounted for by reducing the shear velocity at the top of the mantle under the Indian and Atlantic oceans by about 0·1–0·2 km/s. The difference between the Pacific mantle and the Continental mantle can be explained either by a reduction in shear velocity of the low-velocity layer under the Pacific ocean or by making the low-velocity zone shallower.

1. Introduction

Recently, a comparison of the upper mantle structure under oceans and continents was made by Dorman, Ewing & Oliver (1960) based upon the group velocity of mantle Rayleigh waves. The existence of Gutenberg's low-velocity layer under continents and oceans was confirmed. However, a significant difference in the mantle structure of the Pacific ocean and continents was found. These investigators proposed a model for the sub-Pacific mantle in which the top of the low-velocity layer is located at a shallower depth than in Lehmann's model for the mantle under continents. Since the shallower low-velocity layer may indicate shallower isotherms under the ocean and may consequently explain the unexpectedly large terrestrial heat flow through the ocean basin, it is important to study Rayleigh waves in more detail to compare the upper mantle structure under different oceans and continents.

The upper mantle from the Mohorovičić discontinuity to the bottom of the low-velocity layer controls Rayleigh wave dispersion in the range of period from about 30s to about 200s. Since there is a group velocity maximum in the dispersion curve of Rayleigh waves in the above period range (Ewing & Press 1956), the actual record

* Contribution No. 1018 from the Division of the Geological Sciences, California Institute of Technology.

† Now at the Earthquake Research Institute, Tokyo University, Tokyo, Japan.

starts with an Airy phase, which makes an accurate dispersion analysis difficult. A Fourier method such as applied by Satô (1958) to *G* waves may yield an accurate result. In this paper, we use an alternative method. We start with a layered model of the crust–mantle system, compute the dispersion curve for the model, compute the impulse response seismogram for the dispersion curve, and compare the computed seismogram directly with the actual seismogram. We do not seek phase for phase agreement as much as signal duration, frequency and arrival time correlation. Therefore this is essentially a "group velocity method" with the added advantage of including the Airy phase in the analysis. Eventually when the initial phase of the source and the effect of curvature can be simultaneously allowed for, phase and group agreement between the experimental and theoretical seismograms will reveal the structure with a greater degree of precision and uniqueness. The dispersion curves are computed by Haskell's matrix method programmed for the IBM-704 computer. The computing time is about 3 s per layer per period point. The impulse response seismograms are computed by the Bendix G-15D electronic computer at the Seismological Laboratory, Pasadena.

2. Rayleigh waves across the Indian–Atlantic oceans

Dorman, & others (1960) proposed a model named 8099 for the mantle under the Pacific ocean based on the group velocity of Rayleigh waves obtained by Sutton & others (1960). Aki (1960b) used this model in a study of the mechanism of many circum-Pacific earthquakes, and showed that the model explains very well the actual features of Rayleigh waves propagated through the North and South Pacific oceans. Figure 1 is reproduced from his paper, and shows a comparison of

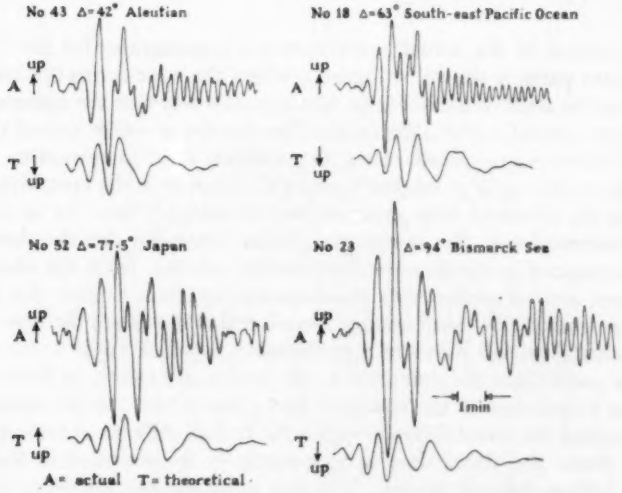

FIG. 1.—Theoretical seismograms of Rayleigh waves based on model 8099 compared with corresponding actual records for Pacific ocean paths.

actual seismograms recorded at Pasadena and the corresponding theoretical seismograms based upon the model 8099. Since he chose earthquakes for which the phase angle of the source function is 0 or π, the observed and theoretical

seismograms agree very well, except that the short period waves riding on the long period waves of the actual records are cut off in the theoretical seismogram.

We made a similar comparison for Rayleigh waves propagated through the Indian and Atlantic oceans, in order to see if model 8099 also applies to these areas. Since we mostly used Pasadena records, the wave paths include continental portions. For these portions, we used a phase velocity curve that is a combination of Press's curve (1960) and the curve of Dorman & others for the Lehmann mantle; the curve is very close to that of model 6EGH which will be described later.

The impulse response seismograms are computed according to the following formula (Aki 1960a),

$$f(t) = \int_{\omega_1}^{\omega_2} \cos\left(\omega t - \frac{\omega\Delta}{c(\omega)} - \phi_{\text{in}}\right) d\omega, \tag{1}$$

where

Δ is the epicentral distance,

ω is the angular frequency,

$c(\omega)$ is the phase velocity without the curvature correction,

ϕ_{in} is the instrumental phase delay,

$\omega_1 = \dfrac{2\pi}{T_1}$ is the higher cut-off frequency with $T_1 = 35$ s, and

$\omega_2 = \dfrac{2\pi}{T_2}$ is the lower cut-off frequency with $T_2 = 200$ s.

A comparison of the actual and theoretical seismograms for the Indian and Atlantic ocean paths is shown in Figure 2 where the wave forms are arranged not according to the absolute arrival time, but in such a way that the agreement is best for the longer period waves. We do this because the absolute arrival time of the theoretical waves are uncertain owing to a possible error in epicentre. The wave group shape, however, is much less susceptible to error in the epicentral distance. We see that the observed Airy phase arrives considerably later (by an amount Δt) than the theoretical one. We cannot exclude the possibility that the observed Airy phase is propagated at the theoretically expected velocity, while the observed long period waves arrived earlier than theoretically expected. Since this possibility seems rather unlikely, we shall assume hereafter that it was not the case.

We studied Rayleigh waves of 7 earthquakes listed in Table 1, for which the great circle paths from the epicentre to the station are shown in Figure 3. The delay in the arrival time of the observed Airy phase relative to the theoretical one is plotted against the travel distance within the Indian–Atlantic oceans in Figure 4. As shown there, the delay time is approximately proportional to the distance within the Indian–Atlantic oceans. This fact indicates that the delay of the Airy phase is actually caused during propagation through the Indian–Atlantic oceans. The delay time is about 6·1 s per 1 000 km. This corresponds to a velocity of the observed Airy phase which is lower than the theoretical one based upon model 8099 by about 0·10 km/s.

The next step is to modify model 8099 to account for the observed low velocity of the Airy phase propagated through the Indian–Atlantic oceans.

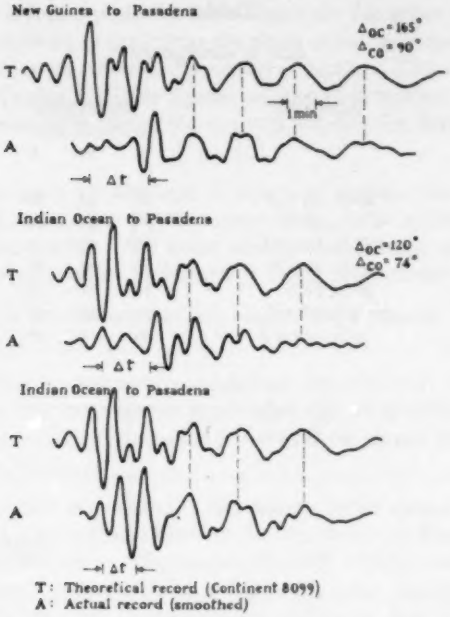

FIG. 2.—Theoretical seismograms of Rayleigh waves based on model 8099 compared with corresponding actual records for Indian–Atlantic ocean paths; Δt is discrepancy in Airy phase time.

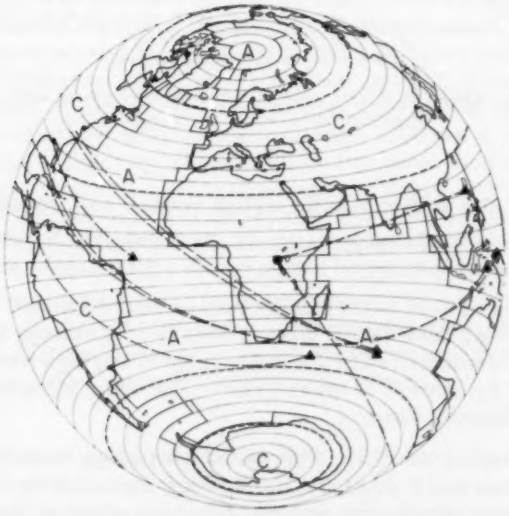

FIG. 3.—Great circle paths across the Indian–Atlantic ocean.

Table 1

List of earthquakes

Date	Epicentre	Origin time (G.C.T.) h	m	s	Region
1958 July 26	40 S, 45·5 E	06	13	50	Indian ocean
1958 Sept. 18	0·5 N, 30 W	14	41	40	Mid-Atlantic
1959 March 1	0·5 S, 134·5 E	16	49	13	New Guinea
1959 June 27	33 S, 179 W	19	04	27	South of Kermadec
1959 July 11	36 S, 78 E	12	01	36	Indian ocean
1959 Aug. 30	36·5 S, 78·5 E	21	45	07	Indian ocean
1960 Jan. 23	4 S, 127·5 E	04	40	56	Ceram Island

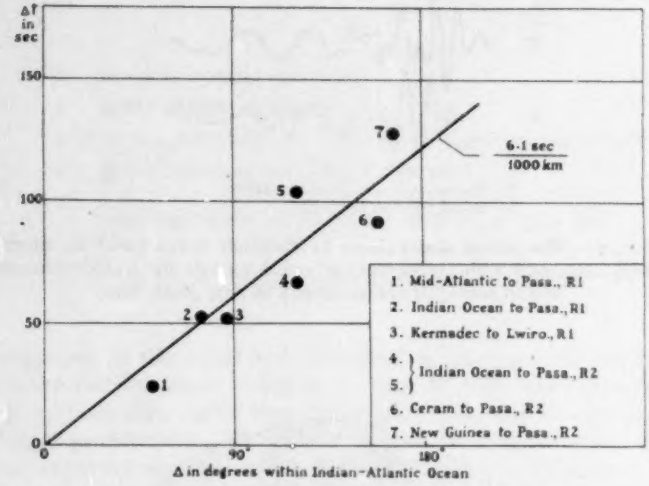

FIG. 4.—Delay in arrival time of observed Airy phase with respect to theoretical time based on the model 8099.

3. Models of the upper mantle under oceans and continents

Before discussing the upper mantle structure under the Indian–Atlantic oceans we shall enumerate here several mantle models relevant to the discussion.

1. Lehmann's model (L). This is based on an unpublished solution by Miss Lehmann, derived from her *S* wave travel-times (Lehmann 1955) for data of stations within continents. The dispersion curve of Rayleigh waves for this model was computed by Dorman & others (1960). The shear velocity distribution for this model is shown in Figure 5.

2. Gutenberg's model (G). This model is based on Gutenberg's study of *S* wave travel-times and is adopted in the Rayleigh wave study by Dorman & others. The shear velocity distribution and the dispersion curve of Rayleigh waves for this model are shown in Figures 5 and 6 respectively.

3. 6EGH. This is based upon the latest result on the shear velocity distribution obtained by Gutenberg (1959) from the slope at the inflection points of the S wave travel-time curves for different hypocentral depths. This model is identical with Press's model (1960) 6EG for depths smaller than 200 km. Case 6EG very well explains the observed Rayleigh wave group velocity for Africa for periods 10 to 70 s.

4. 8099. This is used by Dorman & others to explain the observed group velocity of Rayleigh waves for Pacific ocean paths. The model is obtained by modifying Lehmann's model. The shear velocity distribution and the dispersion curve for this model are shown in Figures 7 and 8 respectively.

5. 6EGHP. This model consists of Gutenberg's mantle (6EGH) and an oceanic crust (Figures 7 and 8).

6. 6EGHP1. This is obtained by modifying case 6EGHP in such a way that the shear velocity at the low-velocity layer takes the same value as that in 8099. The phase and group velocity curves for this model are almost identical with those for 8099 as shown in Figure 10.

The last three models are related to the mantle under oceans. Cases 8099 and 6EGHP1 are almost identical and account for the observed Rayleigh wave group velocity for the Pacific Ocean. The model 6EGHP, which consists of an oceanic crust and Gutenberg's mantle, gives a Rayleigh wave dispersion curve which deviates significantly from the curve for 8099, indicating that Gutenberg's mantle model does not apply to the Pacific ocean basins.

The dispersion tables computed for this paper appear in Figures 12, 13 and 14.

4. Mantle under the Indian–Atlantic oceans

The observed low-velocity of the Airy phase for Indian–Atlantic ocean paths can be explained by a modification of 8099 in which either the shear velocity at the Moho is reduced or the top of the low-velocity layer is raised. In the model 6EGHP1′, the shear velocity at the Moho is reduced by 0·1 km/s as shown in Figure 9. This reduction gives an Airy phase velocity reduced by about 0·05 km/s as shown in Figure 10. For case 8099 mod. 3, the top of the low velocity layer was raised by 19 km compared to 8099, as shown in Figure 9. This modification reduced the Airy phase velocity by about 0·07 km/s, but also lowered the group velocity for periods of 50–125 s as shown in Figure 10. From these cases, and from many others which we have computed, we conclude that the observations can be explained by: (1) assuming lower shear velocity at depths from the Moho to about 50 km by an amount between 0·1 to 0·2 km/s under these oceans than under the Pacific; (2) a combination of (1) together with raising the upper limit of the low-velocity zone. These explanations are consistent with those of Kovach & Press (1960) who studied Rayleigh waves from epicentres in the Indian ocean recorded at the Wilkes station in Antarctica.

5. Use of the wave shape in deducing fine differences in upper mantle structure

So far, we have been concerned primarily with the group arrival time (e.g. the arrival time of the Airy phase) in discussing differences in upper mantle structure.

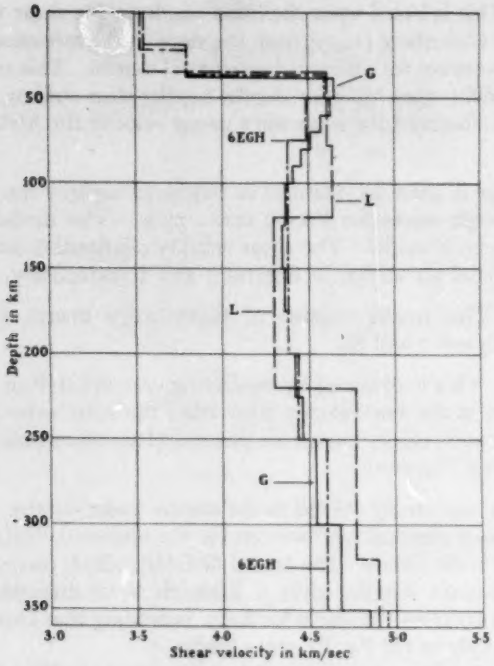

FIG. 5.—Various models of the shear velocity distribution under continents.

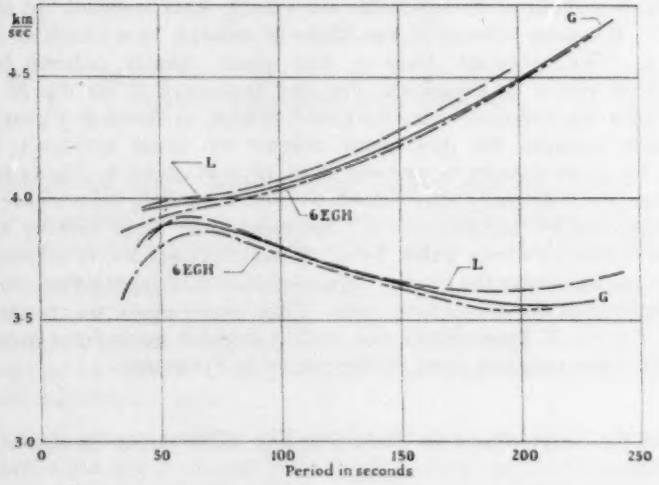

FIG. 6.—Theoretical phase and group velocity of Rayleigh waves for models shown in Fig. 5.

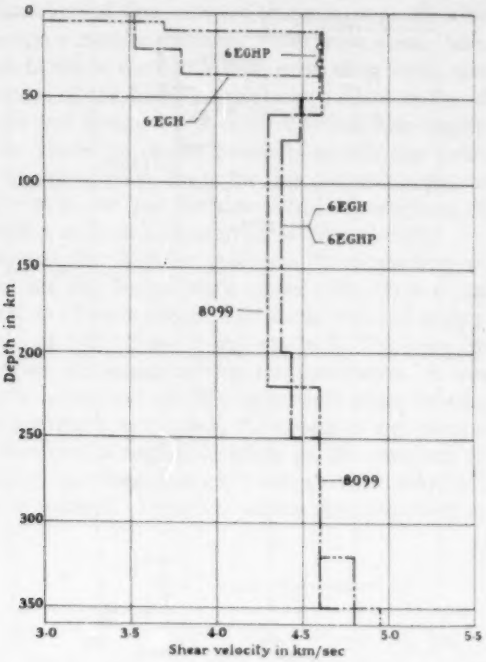

FIG. 7.—Models of shear velocity distribution under oceans.

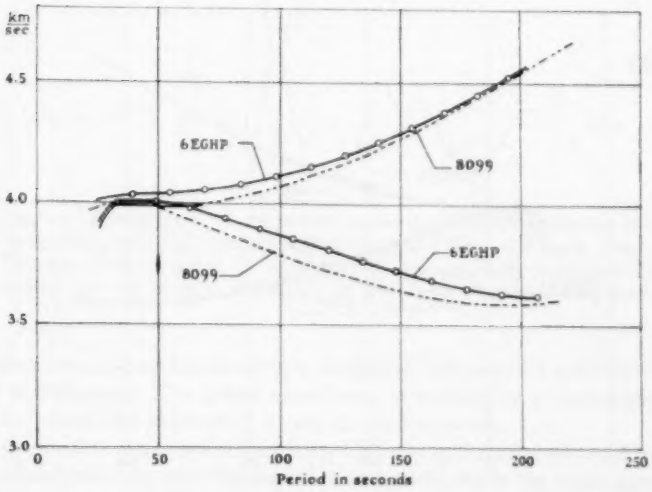

FIG. 8.—Theoretical phase and group velocity of Rayleigh waves for the models shown in Fig. 7.

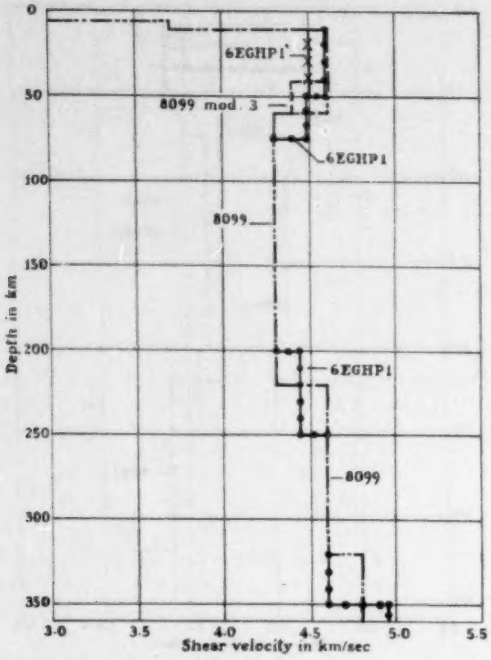

FIG. 9.—Modified models of shear velocity distribution which account for a reduced Airy phase velocity.

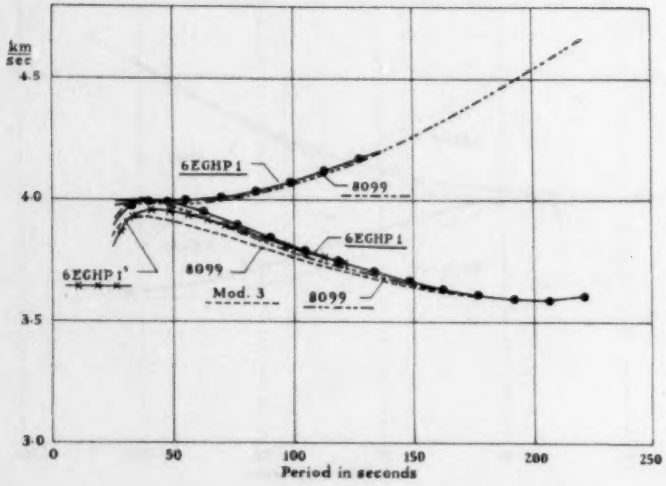

FIG. 10.—Theoretical group velocity of Rayleigh waves for the models shown in Fig. 9.

The use of the phase arrival time or wave shape is more effective in deducing fine differences in the upper mantle structure. The wave shape, however, depends on the space and time factor of the earthquake generating force, and is subject to the effect of the curvature of the Earth's surface as well as to the effect of the "pole shift" (Brune, Nafe and Alsop, 1961), both of which have negligible effect on the group arrival time. Since we cannot precisely specify the earthquake generating force at present the use of wave shape for this purpose is premature. It is, however, of some interest to see how the theoretical seismograms differ between two similar model mantles such as Lehmann's and Gutenberg's.

We shall compute the impulse response $f(t)$ according to Equation 1 for Lehmann's model and for Gutenberg's model (6EGH) and compare them with the Palisades record of a Luzon shock. The shock occurred at 19 h 54 m 45 s G.C.T. on 1959 July 18, at Lat. 15°·5 N and Long. 120°·5 E. The great circle path from the epicentre to Palisades lies mostly within the continents. A small portion of the path is in the Arctic ocean, and we used an oceanic phase velocity for this portion. Since the oceanic portion is very small, the choice of any particular mantle model for this portion produces a negligible effect on the resultant theoretical seismograms. We modified case 8099 in such a way that the velocity of the Airy phase was reduced by 0·10 km/s. Figure 11 shows the theoretical seismograms based

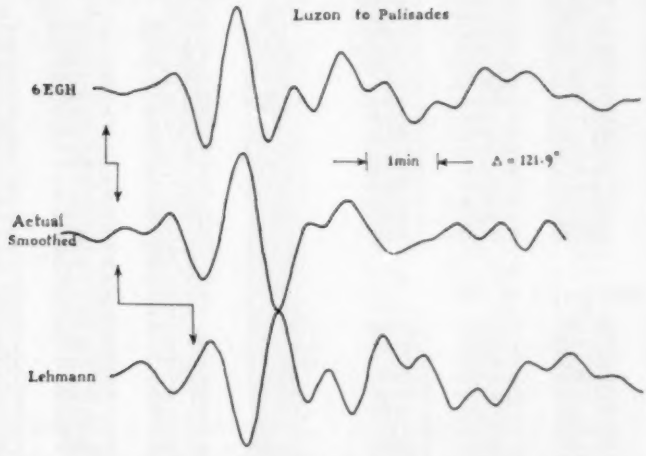

FIG. 11.—Comparison of theoretical seismograms for Lehmann's and Gutenberg's (6EGH) models with Palisades record of Luzon shock. Theoretical seismogram is obtained by tracing dots automatically plotted by the Bendix computer at the Seismological Laboratory.

on Lehmann's model, and Gutenberg's model (6EGH) and the actual seismogram recorded at Palisades. The actual record was smoothed by a symmetric moving average, for which the phase shift is zero at any frequency.

The theoretical seismogram based on Gutenberg's model shows a good peak to peak correspondence with the actual seismogram, while the seismogram based upon Lehmann's model shows a good peak to trough correspondence. This means that due to model differences alone, the phase equalization of Rayleigh waves for

8099 MOD 3

D	ALPHA	BETA	RHO
5.0	1.520	.000	1.030
1.0	2.100	1.000	2.100
5.0	6.410	3.700	2.840
30.0	7.820	4.612	3.340
19.0	8.000	4.400	3.360
160.0	8.170	4.300	3.442
100.0	8.490	4.600	3.526
90.0	8.810	4.800	3.604
90.0	9.320	5.192	3.765
100.0	9.970	5.492	4.010
100.0	10.480	5.790	4.230
100.0	10.850	6.030	4.410
100.0	11.120	6.200	4.545
100.0	11.330	6.315	4.640
100.0	11.490	6.400	4.710
100.0	11.640	6.465	4.770
100.0	11.780	6.531	4.827
100.0	11.920	6.591	4.882
100.0	12.060	6.649	4.940
S-INF.	12.190	6.704	5.000

MODE M 1, 1 N = 20

KD1	T	C	U
.02621	247.616	4.8400	3.6789
.02762	237.941	4.7800	3.6418
.02915	228.333	4.7200	3.6191
.03082	218.723	4.6600	3.6058
.03267	209.036	4.6000	3.5948
.03474	199.192	4.5400	3.5901
.03708	189.104	4.4800	3.5915
.03978	178.678	4.4200	3.5990
.04294	167.795	4.3600	3.6136
.04674	156.312	4.3000	3.6317
.05144	144.037	4.2400	3.6548
.05751	130.695	4.1800	3.6862
.06583	115.834	4.1200	3.7238
.07851	98.557	4.0600	3.7714
.10295	76.286	4.0000	3.8387

MODE M 1, 1 N = 10

KD1	T	C	U
.10296	76.280	4.0000	3.8386
.10855	72.498	3.9920	3.8504
.11539	68.338	3.9840	3.8633
.12416	63.639	3.9760	3.8774
.13626	58.103	3.9680	3.8938
.15576	50.932	3.9600	3.9127
.20272	39.213	3.9520	3.9310
.28388	28.060	3.9440	3.9021
.32458	24.591	3.9360	3.8534
.35099	22.787	3.9280	3.8047

6EGH

D	ALPHA	BETA	RHO
22.0	6.030	3.530	2.780
15.0	6.700	3.800	3.000
13.0	8.000	4.600	3.330
25.0	7.840	4.490	3.350
50.0	7.840	4.380	3.370
75.0	8.020	4.380	3.420
50.0	8.170	4.440	3.490
100.0	8.500	4.600	3.550
100.0	9.000	4.950	3.630
100.0	9.630	5.310	3.890
100.0	10.170	5.630	4.130
100.0	10.580	5.915	4.330
100.0	10.955	6.140	4.490
100.0	11.275	6.285	4.600
150.0	11.460	6.384	4.690
200.0	11.755	6.500	4.800
200.0	12.020	6.610	4.910
200.0	12.280	6.740	5.030
200.0	12.540	6.850	5.130
200.0	12.800	6.960	5.240
200.0	13.020	7.000	5.340
200.0	13.240	7.100	5.440
S-INF.	13.480	7.200	5.540

MODE M 1, 1 N = 23

KD1	T	C	U
.07600	343.168	5.3000	4.1334
.08132	325.650	5.2200	4.0207
.08687	309.577	5.1400	3.9184
.09272	294.638	5.0600	3.8272
.09893	280.565	4.9800	3.7477
.10561	267.125	4.9000	3.6826
.11295	253.894	4.8200	3.5880
.12084	241.326	4.7400	3.5906
.12976	228.593	4.6600	3.5644
.13990	215.727	4.5800	3.5504
.15167	202.528	4.5000	3.5499
.16577	188.655	4.4200	3.5368
.18297	174.074	4.3400	3.5655
.20507	158.228	4.2600	3.6078
.23540	140.484	4.1800	3.6553
.28153	119.755	4.1000	3.7206
.36842	93.331	4.0200	3.7934
.64239	54.614	3.9400	3.8347
1.05098	34.074	3.8600	3.5858
1.31479	27.813	3.7800	3.3362
1.5[illegible]357	24.203	3.7000	3.1540
.35[illegible]0	97.718	4.0313	3.7871
.39571	87.226	4.0048	3.8114
.46305	75.036	3.9783	3.8347
.57420	60.916	3.9518	3.8445
.73324	48.026	3.9254	3.8067
.88158	40.216	3.8989	3.7244
1.00210	35.621	3.8724	3.6286

FIG. 12.—Tabulation of dispersion computations: KD_1 is dimensionless wave number with respect to first layer; D-layer thickness in km, α and β are compressional and shear velocities in km/s; ρ is density in g/cm^3; T is period in s; C and U are phase and group velocity in km/s; Mode $M_{1,1}$ is Rayleigh mode; N-number of layers used in computation.

6EGHP

D	ALPHA	BETA	RHO
5.0	1.520	.000	1.030
1.0	2.100	1.000	2.100
5.0	6.410	3.700	2.840
39.0	8.000	4.600	3.330
25.0	7.840	4.490	3.350
50.0	7.840	4.380	3.370
75.0	8.020	4.380	3.420
50.0	8.170	4.440	3.490
100.0	8.500	4.600	3.550
100.0	9.000	4.950	3.630
100.0	9.630	5.310	3.890
100.0	10.170	5.630	4.130
100.0	10.585	5.915	4.330
100.0	10.955	6.140	4.490
100.0	11.275	6.285	4.600
150.0	11.460	6.384	4.690
200.0	11.755	6.500	4.800
200.0	12.020	6.610	4.910
S-INF.	12.280	6.740	5.030

MODE M 1, 1 N = 19

KD1	T	C	U
.02605	249.172	4.8400	3.6860
.02746	239.346	4.7800	3.6524
.02900	229.535	4.7200	3.6350
.03069	219.660	4.6600	3.6274
.03266	209.110	4.6000	3.6163
.03471	199.342	4.5400	3.6259
.03717	188.684	4.4800	3.6375
.04004	177.512	4.4200	3.6535
.04350	165.639	4.3600	3.6789
.04781	152.813	4.3000	3.7101
.05344	138.638	4.2400	3.7505
.06138	122.440	4.1800	3.8001
.07420	102.772	4.1200	3.8611
.10351	74.754	4.0600	3.9447
.31524	24.915	4.0000	3.8709
.10352	74.748	4.0600	3.9443
.10834	71.507	4.0550	3.9557
.11439	67.810	4.0500	3.9634
.12187	63.727	4.0450	3.9742
.13214	58.850	4.0400	3.9853
.14764	52.737	4.0350	3.9961
.17512	44.516	4.0300	4.0064
.21522	36.266	4.0250	3.9991
.24698	31.642	4.0200	3.9734
.26953	29.030	4.0150	3.9472
.28684	27.313	4.0100	3.9263
.30214	25.962	4.0050	3.8960
.31511	24.924	4.0000	3.8712

MODE M 1, 1 N = 10

KD1	T	C	U
.31516	24.921	4.000	3.8703
.33329	23.612	3.9920	3.8288
.34868	22.615	3.9840	3.7907
.36197	21.829	3.9760	3.7573
.37464	21.133	3.9680	3.7136
.38602	20.551	3.9600	3.6671
.39643	20.052	3.9520	3.6232
.40590	19.624	3.9440	3.5861
.41456	19.254	3.9360	3.5499
.42289	18.913	3.9280	3.5063

6EGHP1

D	ALPHA	BETA	RHO
5.0	1.520	.000	1.030
1.0	2.100	1.000	2.100
5.0	6.410	3.700	2.840
39.0	8.000	4.600	3.330
25.0	7.840	4.490	3.350
50.0	7.840	4.300	3.370
75.0	8.020	4.300	3.420
50.0	8.170	4.440	3.490
100.0	8.500	4.600	3.550
100.0	9.000	4.950	3.630
100.0	9.630	5.310	3.890
100.0	10.170	5.630	4.130
100.0	10.585	5.915	4.330
100.0	10.955	6.140	4.490
100.0	11.275	6.285	4.600
150.0	11.460	6.384	4.690
200.0	11.755	6.500	4.800
200.0	12.020	6.610	4.910
S-INF.	12.280	6.740	5.030

MODE M 1, 1 N = 19

KD1	T	C	U
.02596	249.989	4.8400	3.6897
.02735	240.310	4.7800	3.6337
.02885	230.682	4.7200	3.6128
.03050	221.029	4.6600	3.6020
.03241	210.726	4.6000	3.5858
.03437	201.323	4.5400	3.5916
.03670	191.090	4.4800	3.5975
.03939	180.460	4.4200	3.6070
.04256	169.298	4.3600	3.6256
.04641	157.430	4.3000	3.6487
.05124	144.604	4.2400	3.6799
.05762	130.432	4.1800	3.7174
.06686	114.044	4.1200	3.7651
.08217	94.167	4.0600	3.8315
.13929	56.385	4.0000	3.9738
.08218	94.163	4.0600	3.8310
.08404	92.185	4.0550	3.8383
.08606	90.135	4.0500	3.8456
.08826	87.999	4.0450	3.8535
.09068	85.753	4.0400	3.8615
.09336	83.392	4.0350	3.8702
.09644	80.832	4.0300	3.8796
.09980	78.205	4.0250	3.8900
.10373	75.338	4.0200	3.9013
.10862	72.037	4.0150	3.9144
.11478	68.257	4.0100	3.9282
.12326	63.637	4.0050	3.9463
.13904	56.488	4.0000	3.9740

MODE M 1, 1 N = 10

KD1	T	C	U
.13904	56.487	4.000	3.9741
.31325	25.123	3.9920	3.8947
.33534	23.515	3.9840	3.8493
.35342	22.357	3.9760	3.7936
.36831	21.496	3.9680	3.7445
.38093	20.826	3.9600	3.7032
.39207	20.276	3.9520	3.6663
.40204	19.813	3.9440	3.6342
.41210	19.368	3.9360	3.5728
.42082	19.005	3.9280	3.5294

FIG. 13.—Tabulation of dispersion computations (notation as for Fig. 12).

this path would yield source functions which have opposite sense for the two models.

In Figure 11, the seismograms are arranged not according to the absolute time but in such a way as to obtain the best fit between the actual and theoretical waves. The time shift required to obtain the best fit is indicated by arrows in Figure 11. The shift of about 1 minute in Lehmann's case is probably too great to be accounted for by an error in the epicentre location.

6EGHP1'

D	ALPHA	BETA	RHO
5.0	1.520	.000	1.030
1.0	2.100	1.000	2.100
5.0	6.410	3.700	2.840
39.0	8.000	4.500	3.330
25.0	7.840	4.490	3.350
50.0	7.840	4.300	3.370
75.0	8.020	4.300	3.420
50.0	8.170	4.440	3.490
100.0	8.500	4.600	3.550
100.0	9.000	4.950	3.630
100.0	9.630	5.310	3.890
100.0	10.170	5.630	4.130
100.0	10.585	5.915	4.330
100.0	10.955	6.140	4.490
100.0	11.275	6.285	4.600
150.0	11.460	6.384	4.690
200.0	11.755	6.500	4.800
200.0	12.020	6.610	4.910
S-INP.	12.280	6.740	5.030

MODE M 1, 1 N = 19

KD1	T	C	U
.02590	250.577	4.8400	3.7155
.02729	240.873	4.7800	3.6310
.02878	231.254	4.7200	3.6096
.03042	221.615	4.6600	3.5984
.03232	211.326	4.6000	3.5818
.03426	201.952	4.5400	3.5872
.03657	191.751	4.4800	3.5926
.03923	181.162	4.4200	3.6016
.04237	170.055	4.3600	3.6197
.04617	158.258	4.3000	3.6418
.05096	145.387	4.2400	3.6701
.05714	131.522	4.1800	3.7085
.06597	115.581	4.1200	3.7535
.08039	96.254	4.0600	3.8141
.11721	67.005	4.0000	3.9130

MODE M 1, 1 N = 10

KD1	T	C	U
.11709	67.074	4.0000	3.9136
.13113	60.015	3.9920	3.9357
.16450	47.938	3.9840	3.9641
.23831	33.156	3.9760	3.9372
.27360	28.938	3.9680	3.8881
.29747	26.669	3.9600	3.8466
.31643	25.122	3.9520	3.8101
.33289	23.928	3.9440	3.7706
.34730	22.982	3.9360	3.7335
.36037	22.194	3.9280	3.6943

FIG. 14.—Tabulation of dispersion computations (notation as for Fig. 12).

This comparison implies at least that Gutenberg's model 6EGH explains Rayleigh wave propagation across the continents as well as Lehmann's model. Since model 8099 for the sub-Pacific mantle was obtained by a modification of Lehmann's mantle, Dorman & others emphasized the difference in the depth of the top of the low-velocity layer under the continental and oceanic mantle. If we start with Gutenberg's model (6EGH) in constructing the mantle under the Pacific ocean, the required modification (6EGHP1) is not in the depth of the top of the

low-velocity zone but in the value of the shear velocity at the lowest velocity layer (4·30 km/s under the ocean against 4·38 km/s under the continent). Thus the difference in upper mantle under the Pacific Ocean and continents can be explained by a change in velocity in the low-velocity zone as well as by extending the low-velocity zone upward.

6. Acknowledgments

This research was supported by Contract No. AF-49(638)910 of the Air Force Technical Application Centre as part of the Advanced Research Projects Agency, project Vela.

Seismological Laboratory,
California Institute of Technology,
Pasadena, California:
1961 *January*

References

Aki, K., 1960a. Study of earthquake mechanism by a method of phase equalization applied to Rayleigh and Love waves, *J. Geophys. Res.* **65,** 729–740.

Aki, K., 1960b. Interpretation of source functions of circum-Pacific earthquakes obtained from long period Rayleigh waves, *J. Geophys. Res.*, **65,** 2405–2417.

Brune, J. N., Nafe, J. E., & Alsop, L. E., 1961. The polar phase shift of surface waves on a sphere, *Bull. Seismol. Soc. Amer.*, **51,** 247–258.

Dorman, J., Ewing, M., & Oliver, J., 1960. Study of shear velocity distribution in the upper mantle by mantle Rayleigh waves, *Bull. Seismol. Soc. Amer.*, **50,** 87–115.

Ewing, M., & Press, F., 1956. Rayleigh wave dispersion in the period range 10 to 500 seconds, *Trans. Amer. Geophys. Un.*, **37,** 213–215.

Gutenberg, B., 1959. The asthenosphere low-velocity layer, *Annali di Geofisica*, **12,** 439–460.

Kovach, R. L., & Press, F., 1961. Rayleigh wave dispersion and crustal structure in the eastern Pacific and Indian oceans, *Geophys. J.*, **4,** 202–216.

Lehmann, I., 1955. The times of *P* and *S* in North-Eastern America, *Annali di Geofisica*, **8,** 351–370.

Press, F., 1960. Crustal structure in the California–Nevada region, *J. Geophys. Res.*, **65,** 1039–1051.

Sutton, G. H., Ewing, M., & Major M., 1960. Rayleigh wave group velocity extrema, reported at the Helsinki meeting of the International Association of Seismology and Physics of the Earth's Interior.

The Correlation of Radio Star Scintillations with Geomagnetic Disturbances

B. H. Briggs

(Received 1961 February 8)

Summary

The correlation between the degree of scintillation of the radio source Cassiopeia *A* and the local magnetic *K*-index is studied. It is shown that the correlation coefficient between these quantities depends upon the epoch of the solar cycle at which the observations are made, on the position of the source in the sky, and on the radio frequency used. For observations on 38 Mc/s made at sunspot minimum, the correlation coefficient is small but positive for all positions of the source. At sunspot maximum, the correlation coefficient is positive when the source is near upper transit and negative when it is near lower transit; the average value of the correlation coefficient for all positions of the source is approximately zero. It is shown that these results can be explained when the finite angular diameter of the radio source is taken into account. For some conditions an increase in the degree of irregularity of the ionosphere can result in a decrease in the degree of scintillation which is observed. It is suggested, therefore, that the degree of irregularity of the ionosphere always increases during magnetic disturbances in medium latitudes, and that the negative values of the correlation coefficient between scintillation index and magnetic *K*-index which are sometimes obtained are due to a secondary effect related to the finite size of the source. The results of the present paper explain the inconclusive and conflicting results of earlier workers.

1. Introduction

Regular observations of the degree of scintillation of the radio source Cassiopeia *A* were made during 1957 and 1958 at Cambridge (52°N, 0°W) and Jodrell Bank (53°N, 2°W) as part of the programme for the International Geophysical Year. The Cambridge observations were made on a frequency of 38 Mc/s and those at Jodrell Bank on a frequency of 79 Mc/s. The observations at both places were a continuation of earlier work and the methods of observation have been described in earlier papers (e.g. Ryle & Hewish 1950; Dagg 1957). The records are of the intensity of the source (i.e. the square of the amplitude) and the degree of scintillation is conveniently given by expressing the depth of scintillation on the record as a fraction of the mean source intensity. At Cambridge an index on a scale 0 to 5 is used to express this quantity, while at Jodrell Bank the results

are given as percentages of the mean source intensity; the measurements are of essentially the same quantity, and for brevity we shall refer to both as "scintillation indices". The scintillations have been shown to be produced by irregularities of ionization in the ionosphere, the main effect being due to the F Region.

It appeared that the observations made on the two frequencies during the International Geophysical Year, a period of exceptionally high solar activity, would be very suitable for a detailed investigation of the relation of radio star scintillations to magnetic disturbances. Previous work on this relationship has been inconclusive and to some extent conflicting. Thus Hewish (1952) found no correlation between the scintillation index observed at Cambridge during 1949–50 and the occurrence of magnetic storms. On the other hand Dagg (1957), observing at Jodrell Bank during 1955, showed that for a number of individual magnetic disturbances the scintillation index increased and was quite closely related to changes in the horizontal component of the magnetic field. When the magnetic *K*-index was used as an index of disturbance, however, and all the results were taken together, the overall correlation was found to be zero. Hartz (1955), observing scintillations of the same source at Ottawa (45°N, 75°W) and using a frequency of 54 Mc/s, found only a very small positive correlation between the occurrence of scintillations and the magnetic *K*-index.

The fact that no clear positive correlation is found between the scintillation index and the magnetic *K*-index is surprising for the following reason. It has been shown that there is a close correlation between the occurrence of scintillations and the presence of diffuse reflections from the F Region of the ionosphere, when observed by the echo-sounding method. This condition is usually referred to as "Spread F" (e.g. Ryle & Hewish 1950; Little & Maxwell 1951; Briggs 1958a). It is therefore reasonable to suppose that the same ionospheric irregularities are responsible for both phenomena. Also, it has been shown that in medium latitudes there is a strong positive correlation between the occurrence of spread F echoes and the magnetic *K*-index (Shimazaki 1959; Lyon, Skinner & Wright 1960). Thus, the degree of irregularity of the ionosphere almost certainly increases during magnetic disturbances, and it is difficult to account for the lack of correlation between radio star scintillations and magnetic *K*-index.

The results of the present investigations are presented in Section 2. It is shown that the correlation coefficient between the scintillation index and the magnetic *K*-index is different for the two radio frequencies (38 and 79 Mc/s) and also depends upon the position of the source in the sky. For observations made on 38 Mc/s, the correlation coefficient is found to be positive when the source is near upper transit, and negative when the source is near lower transit. In view of this surprising result, the work was extended to include the sunspot minimum period. For this purpose, observations made at Cambridge during 1954–5 were used. It is found that for sunspot minimum the correlation coefficient is small but positive for all positions of the source. A possible explanation of these results is discussed in Section 4, where it is suggested that the scintillation index may be influenced by the fact that the radio source has a finite angular diameter. The importance of this effect varies with the position of the source and the degree of irregularity of the ionosphere, and it is shown that these variations can readily account for the fact that the correlation coefficient of the scintillation index with the magnetic *K*-index is sometimes positive and sometimes negative. The same effect would be expected to modify the mean diurnal variation of the scintillation index, and this point is considered in Section 3.

We shall not be concerned in the present paper with the *rate* of scintillation of the radio source, but it may be noted in passing that there is general agreement that in medium latitudes the rate increases during periods of magnetic disturbance. This is readily explained, since it is known that the drift velocity of the irregularities in the ionosphere increases during magnetic disturbances (Briggs & Spencer 1954). Thus, the irregular diffraction pattern formed on the ground is carried more rapidly past the observing receiver, and the scintillation rate is increased. The high correlation which exists between the scintillation rate and the magnetic *K*-index is probably not significant when the origin of the irregularities is in question, though it is of interest in connection with their *movements*. In contrast, any correlation which may be found between the *intensity* of the ionospheric irregularities and the magnetic *K*-index is important in the discussion of theories of the origin of the irregularities.

2. The correlation between the scintillation index and the magnetic *K*-index

In evaluating the correlation coefficient between two quantities like the scintillation index and the magnetic *K*-index, it is important to consider the effect of periodic variations and trends. Both quantities have diurnal and seasonal variations, and also vary with the sunspot cycle. The diurnal variation alone, which is similar for the two quantities with a maximum near midnight, would produce a positive correlation coefficient between the two quantities. This would not necessarily imply any close relation between the quantities, since many other quantities have a similar diurnal variation (e.g. ground temperature). It is therefore desirable to remove the mean diurnal variations before the correlation coefficient is calculated, or alternatively to calculate the correlation in such a way that the diurnal variation has no effect. Similar remarks apply to seasonal, sunspot cycle, and any other long period variations which may be present.

In the present work, these variations were eliminated in the following way. Firstly, the data for each month were considered separately. This in itself was considered to be sufficient to eliminate seasonal and sunspot cycle variations. Secondly, the correlation coefficients were evaluated at fixed times of day by using the values for each day of the month. This meant that each value of correlation coefficient was calculated from about thirty pairs of values of scintillation index and *K*-index. The correlation determined in this way is between the day to day fluctuations of both quantities from their monthly mean values at fixed times of day. A disadvantage of this method is that the error of each value of correlation coefficient is rather large (about $\pm 0{\cdot}18$), but it has the advantage that the variation of the correlation coefficients with solar time and with the hour angle of the source can be investigated.

Magnetic *K*-indices from the magnetic observatory at Hartland (51°N, 4°W) were used. As these are given at three-hourly intervals, it was necessary to work with this interval throughout the analysis. The first step, therefore, was to work out three-hourly averages of the scintillation indices, which are given at hourly intervals for Cambridge and half-hourly intervals for Jodrell Bank. The intervals were centred on 01.30, 04.30, 07.30, 10.30, 13.30, 16.30, 19.30 and 22.30 G.M.T. The correlation coefficients between the three-hourly averages of the scintillation indices and the corresponding *K*-indices were then calculated from the standard formula. In order to investigate the dependence of the correlation coefficient on

the hour angle of the source, a mean value for the difference between solar time and hour angle was used for each month. This difference is in error by ± 1 hr at the beginning and end of the month, but this error is not considered to be important for the present purpose. Values of the scintillation index were not available for every hour owing to equipment limitations; in particular data for most of the daylight hours are missing in the Cambridge results owing to the serious interference from distant radio stations which is experienced on the frequency of 38 Mc/s in the day time. However, all values of the hour angle of the source are obtained in the course of a year. The data for Jodrell Bank were more continuous, with only occasional missing values, but in order to permit a valid comparison between the results obtained from the two sets of data, values of the index were only used when they were available for *both* stations.

The results for 1958 (the later part of the I.G.Y.) are shown in Figure 1(a) (Cambridge, 38 Mc/s) and Figure 1(b) (Jodrell Bank, 79 Mc/s). The individual

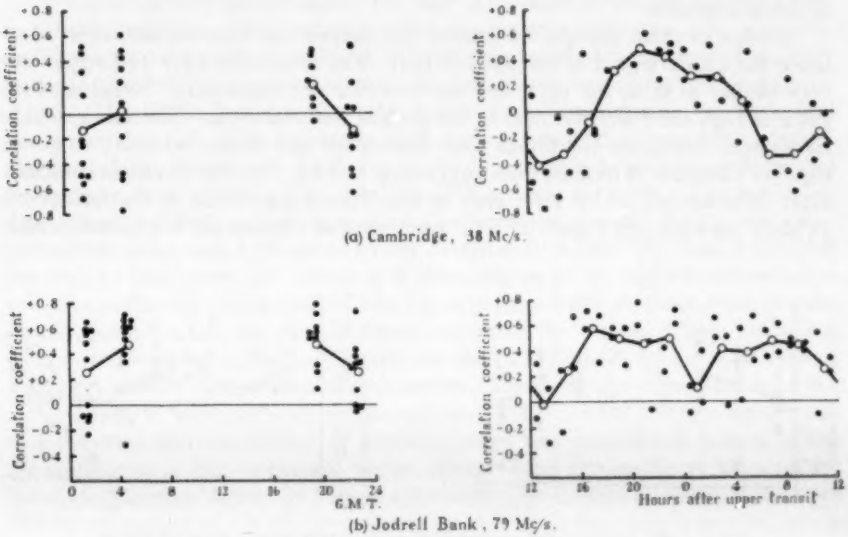

FIG. 1.—The values of the correlation coefficient between the scintillation index and the magnetic *K*-index, plotted as functions of solar time, and of the hour angle of the source. (a) Cambridge, 38 Mc/s. (b) Jodrell Bank, 79 Mc/s. Results for 1958 (mean sunspot number 185).

monthly values of correlation coefficient are plotted as functions of solar time and of the hour angle of the source. Also the mean values of groups of points are shown, and these mean values are joined by straight lines.

Owing to the absence of points during the daytime, no significant conclusions can be drawn from the solar plots, though there does seem to be a tendency for the correlation coefficient to have a minimum value at midnight. When the results are plotted as functions of the hour angle of the source, however, some interesting and significant variations become apparent. The clearest variation occurs for the 38 Mc/s results, for which the correlation coefficient is negative when the source is near lower transit, and positive when it is near upper transit; the mean value of

the correlation coefficient for all the results taken together is approximately zero. The results for 79 Mc/s show a somewhat similar though less marked variation. The mean value of the correlation coefficient is approximately zero near lower transit and has a positive value of about +0·5 near upper transit; the mean value for all the results taken together is $+0{\cdot}36 \pm 0{\cdot}02$.

In considering the significance of these results, it is necessary to remember that the line of sight to the source intersects the ionosphere in a point whose latitude varies with the position of the source in the sky. This point is at its highest possible latitude when the source is at lower transit. For the Cassiopeia source, the effective region of the ionosphere for the production of scintillations is quite close to the auroral zone when the source is near lower transit. On these grounds, a higher correlation might have been expected between scintillation index and *K*-index when the source is near lower transit than when it is near upper transit. This is exactly the opposite of the variation obtained. Thus, the results cannot be explained on the basis of the changing geographical position of the effective region of the ionosphere.

In view of these unexpected results, the analysis was repeated for other years, using the Cambridge data for 38 Mc/s only. The results for 1957 and 1959 were very similar to those for 1958, and are therefore not reproduced. These were all years of high solar activity, near to the peak of the solar cycle. The data available for sunspot minimum conditions were incomplete and it was necessary to group together a number of months from 1953, 1954, and 1955 in order to obtain sufficient data. The results, which refer only to the observations made at Cambridge on 38 Mc/s, are shown in Figure 2. The mean sunspot number for the months which

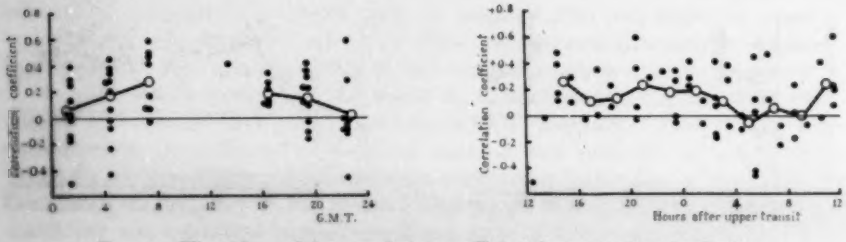

FIG. 2.—The values of the correlation coefficient between the scintillation index and the magnetic *K*-index, plotted as functions of solar time and of the hour angle of the source. Cambridge, 38 Mc/s. Results for 1953, Aug., Sept., Oct., Dec.; 1954, Jan., Feb., Sept., Dec.; 1955, March, June, Aug. (mean sunspot number 13).

were used was 13. The results may be compared with those shown in Figure 1 for 1958, for which year the mean sunspot number was 185. It will be seen that at sunspot minimum there is no significant variation of the correlation coefficient with the hour angle of the source. All but one of the mean values are positive, though the values are very small; the mean value of the correlation coefficient for all the results taken together is $+0{\cdot}10 \pm 0{\cdot}02$.

From all the above results, the conclusion is reached that a clear correlation between the scintillation index and the magnetic *K*-index exists only at sunspot maximum, and that it varies with the position of the source and with the frequency used. In particular, for observations on 38 Mc/s, the correlation coefficient

is positive when the source is near upper transit and negative when the source is near lower transit. It is now clear why earlier workers obtained inconclusive or contradictory results since they did not separate the results according to the epoch of the solar cycle and the hour angle of the source. Since a positive correlation is expected for the reason already discussed, it is reasonable to suppose that the negative values obtained when the source is near lower transit are in some way anomalous, and produced by the intrusion of some secondary effect.

In Section 4 a suggested explanation of these negative values will be given, based upon the idea that they are due to the effect of the finite size of the radio source. However we shall first present a related piece of evidence concerning the mean diurnal variation of the scintillation index, which also shows an anomaly when the source is near lower transit.

3. The monthly mean diurnal variation of scintillation index

Previous workers have discussed the diurnal variation of the scintillation index, and drawn attention to the maximum which usually occurs at a time near midnight. In Figure 3 the Cambridge results for 38 Mc/s are presented in the form of monthly mean curves for 1954 (near sunspot minimum) and for 1958 (near sunspot maximum). The results for 1954 show the expected maximum during the night and low values by day. The results for 1958 show a new and unexpected variation. For Jan., Feb., March and April, the night time peak is large in magnitude and has become double, with a well defined minimum near midnight. The curves for Oct., Nov., and Dec., are rather similar. The remaining months show a very complicated variation with high values by day as well as by night. The feature to which we wish to draw particular attention is the splitting of the night-time maximum into two peaks. It will be noticed that the minimum between these peaks is most clearly defined when the time of lower transit of the source is near midnight. (Times of lower transit for each month are shown in Figure 3 by the short vertical lines). A careful examination of the curves shows that the minimum does not occur exactly at midnight or at the time of lower transit, but at a time roughly midway between these two times. A similar though less pronounced feature in the diurnal curves is also noticeable in the Jodrell Bank results for 79 Mc/s, as reported by Chivers (1960). In Figure 4 the results for the two frequencies for 1958 March are compared. It will be noticed that the dip in the curve near midnight is narrower and less deep on the higher frequency.

It is difficult to believe that this secondary minimum during the night, clearly associated in some way with the time of lower transit of the source, really represents a decrease in the effect of the ionosphere on the radio waves. When the source is near lower transit, the thickness of the ionosphere along the line of sight has its maximum value, and it would be expected that the irregularities in the ionosphere would then have their maximum effect. The results suggest that some secondary effect is causing the scintillation index to decrease when the disturbing effect of the ionosphere becomes very large. If this secondary effect were absent, the diurnal curve for 38 Mc/s might be approximately as shown by the dotted line in Figure 4 and this line would represent the true disturbing effect of the ionosphere. If this is accepted, it follows that between the points marked (a) and (b) an increase in the degree of irregularity of the ionosphere causes a decrease of the scintillation index. The negative correlation coefficient between the scintillation index and the magnetic K-index obtained when the source is near lower transit could then be

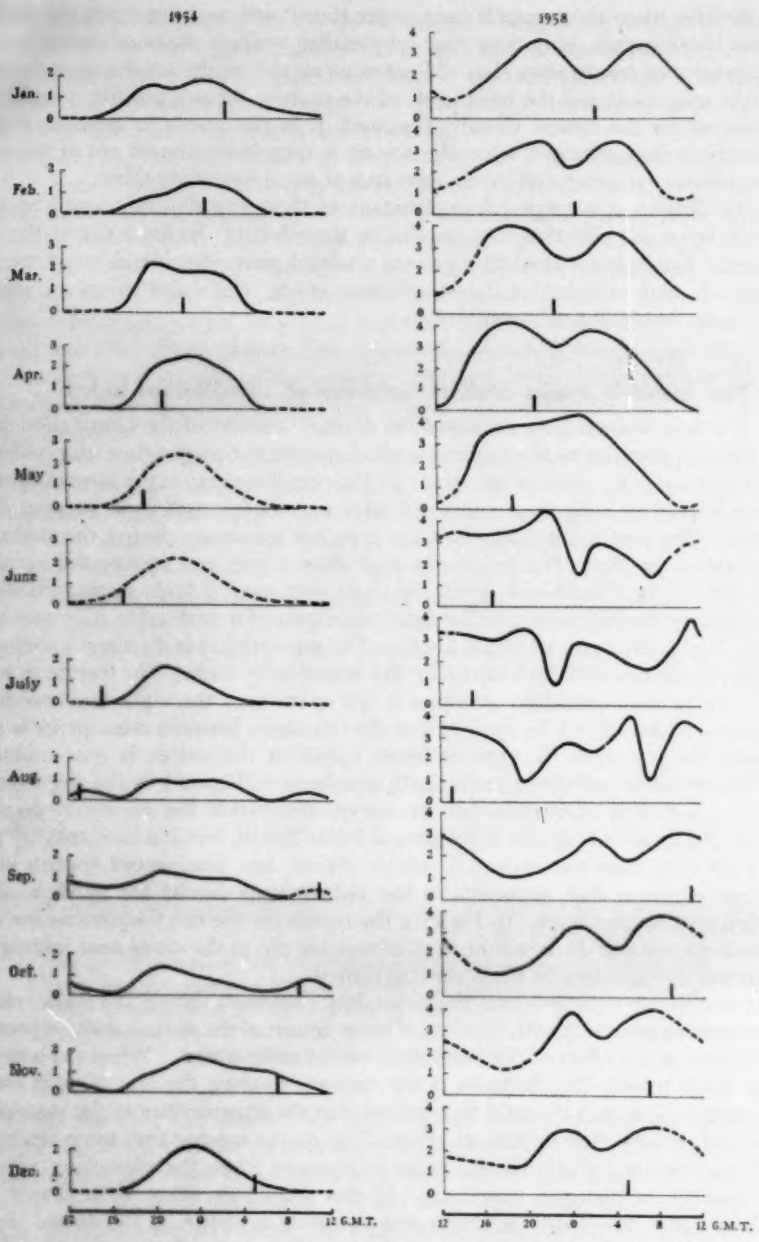

FIG. 3.—Monthly mean diurnal variations of scintillation index for 1954 and 1958. Cambridge, 38 Mc/s. The dotted parts of the curves are uncertain owing to the small number of observations made at these times.

explained if it is supposed that the degree of irregularity of the ionosphere increases with increasing K-index. The results for both frequencies (Figure 1) are qualitatively just as would be expected.

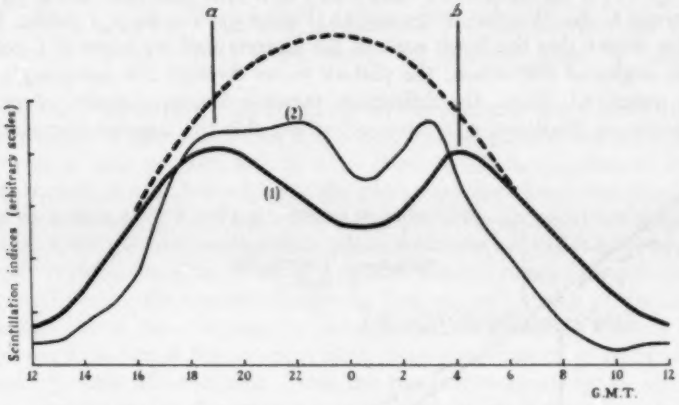

FIG. 4.—Diurnal variations of scintillation index for 1958, March. (1) Cambridge, 38 Mc/s. (2) Jodrell Bank, 79 Mc/s.

4. A suggested explanation of the results: the effect of the finite size of the radio source

The first suggestion that the degree of scintillation of a radio star may be reduced because of its finite size appears to have been made by Little (private communication). The amplitude of scintillation of the source in Cassiopeia, observed at the Geophysical Institute of the University of Alaska, was found to be less than for the source in Cygnus, when both were observed at the same angle of elevation. A similar result has been reported by Chivers (1960), observing at Jodrell Bank. Now the Cassiopeia source is approximately circular in shape with an angular diameter of about 4 minutes of arc (Baade & Minkowski 1954). The Cygnus source is believed to consist of two small objects each subtending about 1 minute by 0·5 minutes of arc (Jennison & Latham 1959). Thus, the two sources differ considerably in solid angle, and if the different parts of the larger Cassiopeia source scintillate independently, the fluctuations will tend to cancel out. This effect is, of course, the radio analogue of the well known optical effect that stars show scintillations but planets do not.

In the present work, only the Cassiopeia source is observed. Whether the finite size of this source is important or not depends upon the size of the ionospheric irregularities and their distance from the observer. We shall now discuss this point with a view to explaining the results obtained in Section 2 and Section 3.

In Figure 5, the ionospheric irregularities of size L are assumed to be concentrated in a layer at a height h above the ground. Let ϕ_1 be the root-mean-square phase deviation produced across the wavefront of a wave which traverses this layer at normal incidence. If the angle of incidence is i, the length of path through the irregularities is increased by a factor sec i. Now the root-mean-square phase deviation is proportional to the square root of the length of the path through the irregular

medium (Fejer 1953; Briggs 1958b), and so the phase deviation ϕ_0 for an angle of incidence i is given by

$$\phi_0 = \phi_1(\sec i)^{\frac{1}{2}}. \tag{1}$$

Now consider the irregular diffraction pattern produced near the ground on a plane normal to the direction of the source (Figure 5). For $\phi_0 > 1$ radian, Hewish (1951) has shown that the linear scale of the pattern is of the order of L/ϕ_0. Also, for small angles of diffraction, the pattern turns through the same angle as the incident radiation. Thus, the diffraction patterns due to opposite edges of the radio source are displaced a distance $z\theta$, where θ is the angular diameter of the

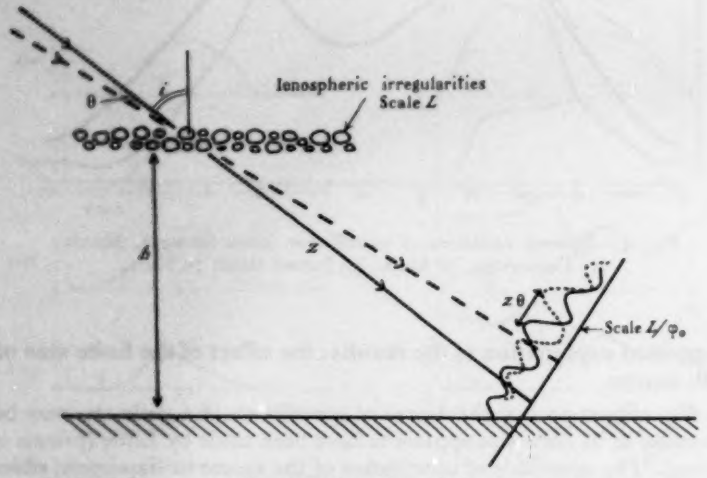

FIG. 5.—Diagram to illustrate the effect of the finite angular diameter of the radio source.

source and z the distance from the irregularities to the observer. For the amplitude of scintillation to be significantly reduced due to the finite size of the source this displacement must be of the same order as the scale of the pattern, that is

$$z\theta \sim L/\phi_0. \tag{2}$$

If the curvature of the earth is neglected, we have $\sec i = z/h$. Thus, using (1) the condition (2) may be written

$$\phi_1(\sec i)^{\frac{1}{2}} \sim L/(h\theta). \tag{3}$$

For given values of L, h, and θ, the effect of the finite size of the source will become important when $\phi_1(\sec i)^{\frac{1}{2}}$ is large enough to satisfy equation (3). Thus, the effect is likely to be more important when the ionosphere is very irregular (ϕ_1 large), and more important when the source is near lower transit ($i = 70°$) than when it is near upper transit ($i = 6°$).

The order of magnitude of the quantity $L/(h\theta)$ will now be estimated. The irregularities are known to be elongated (Spencer 1955, Jones 1960), and for the present purpose it is their smallest dimension which is relevant. In the work of Jones (1960), the sizes of the irregularities were represented by the distance at

which an auto-correlation function had fallen to one-half, and a typical value for this quantity, measured along the smallest dimension, was 1 km. The values of L to be used in equation (3) should be a length which is more characteristic of the separation between maxima, and this will be about four times the distance determined by Jones. We therefore take $L = 4$ km. For the height h a mean value of 350 km will be assumed. The angular diameter θ of the source Cassiopeia A is about $1{\cdot}2 \times 10^{-3}$ radian. With these values, the quantity $L/(h\theta)$ is found to be approximately 10.

We can now see whether the finite size of the source is likely to be important. When the source is near upper transit equation (3) shows that it would be necessary for ϕ_1 to be at least 10 radians before the effect would be significant. However, when the source is near lower transit, the same equation shows that the necessary value of ϕ_1 is then only 2 radians. Previous work (Hewish 1952) has shown that a typical value for the root-mean-square phase deviation on 38 Mc/s for moderately disturbed conditions is of the order of 1 radian. For the more disturbed conditions encountered during the sunspot maximum year of 1958, values of the order of a few radians would be a reasonable assumption. It therefore appears that the effect of the finite size of the source is likely to be important on 38 Mc/s only when the source is near lower transit. Now the root-mean-square phase deviation is inversely proportional to the frequency, and so for 79 Mc/s any effects which may be attributed to the finite size of the source are likely to be less pronounced, and to be confined even more closely to the time of lower transit.

In general, the effect will be a maximum when the quantity $\phi_1(\sec i)^{\frac{3}{2}}$ is a maximum. Now ϕ_1 reaches a maximum at some time near midnight, but $(\sec i)^{\frac{3}{2}}$ is a maximum at the time of lower transit. Thus the greatest effect will be observed when lower transit occurs at midnight, because both terms then reach their maximum values simultaneously. If lower transit is not at midnight, the greatest effect will be observed at some time between the time of lower transit and midnight, when $\phi_1(\sec i)^{\frac{3}{2}}$ is a maximum.

To explain the results of Section 2, it is only necessary to note that when the source is near lower transit there will be occasions when an increase in the degree of irregularity of the ionosphere (i.e. in ϕ_1) will enable equation (3) to be satisfied when previously it was not, and will therefore result in a decrease in the amplitude of the scintillation. Thus, if the irregularity of the ionosphere increases with increasing magnetic K-index, the correlation between scintillation index and K-index may, nevertheless, be negative. This effect will be more pronounced on 38 Mc/s than on 79 Mc/s. The results (Figure 1) show that on 38 Mc/s the correlation is negative for a considerable period around the time of lower transit. On 79 Mc/s however, the individual values of the correlation coefficient for the times near lower transit are sometimes positive and sometimes negative, with a mean value of approximately zero. This is just the type of result which would be expected. At sunspot minimum the effect disappears, probably because ϕ_1 is never large enough for equation (3) to be satisfied, even near lower transit.

The results of Section 3 can also be explained by the decrease of scintillation index when the finite size of the source becomes important. The main features of the curves (Figures 3 and 4) are as would be expected, including the time at which the subsidiary minimum occurs. As previously mentioned, this minimum occurs between the times of lower transit and midnight, and is most pronounced when these times coincide. It is absent at sunspot minimum.

5. Further discussion

It has been shown that the finite size of the Cassiopeia source can explain the unexpected results obtained when the correlation of the scintillation index with the magnetic K-index is studied. It seems likely that for latitudes near 50°, the degree of irregularity of the ionosphere always increases during magnetic disturbances, and that the negative values of the correlation coefficient which are sometimes obtained when the source is near lower transit are due to this secondary effect related to the size of the source.

It should be mentioned that at low latitudes, within 20° of the equator, radio star scintillations and spread F echoes are *both* negatively correlated with the magnetic K-index (Wright, Koster & Skinner 1956; Koster & Wright, 1960; Shimazaki 1959a, b; Lyon, Skinner & Wright 1960). Thus, near the equator, the degree of irregularity of the ionosphere decreases during magnetic disturbances, in contrast to the increased irregularity at higher latitudes.

It appears from the present results that the scintillation index of the Cassiopeia source as measured on 38 Mc/s is not a very useful measure of the degree of irregularity of the ionosphere. Results obtained on 79 Mc/s are more reliable in this respect, but even on this frequency the finite size of the source is sometimes important. The degree of irregularity of the ionosphere is probably not very well represented by the mean diurnal curves of scintillation index of the type shown in Figure 3, and theories of the origin of the irregularities should be not based upon their detailed shapes as was, for example, the theory of Harrower (1957a, b).

In an earlier paper, (Briggs 1958a) the correlation between the scintillation index and the spread F echoes observed in vertical sounding of the ionosphere was studied. It was shown that the highest correlation was obtained when the ionospheric observing station was directly below the irregularities which lay in the line of sight to the source. This result was as might have been expected, and it was used to make deductions about the sizes of the patches of irregularities. These results were for 1954 and 1955, a period near sunspot minimum. When the calculations were repeated for a period near sunspot maximum, a completely different result was obtained. When the source was near lower transit, the correlation between scintillation index and spread-F index was often negative, even when the observing station was almost directly beneath the irregularities. It is clear that this result can also be explained as due to the finite size of the source. Under such conditions, the spread-F index is a more reliable index of the degree of irregularity of the ionosphere than is the scintillation index.

Acknowledgments

The observations of the scintillation index of the radio source Cassiopeia *A* were made at Jodrell Bank and Cambridge during 1957 and 1958 as part of the programme of the British National Committee for the International Geophysical Year. I am grateful to the workers at Jodrell Bank for making their results available. The analysis described in this paper was carried out as part of a programme of work on ionospheric irregularities, supported by a grant from the Department of Scientific and Industrial Research.

Cavendish Laboratory,
Cambridge.
1961 *January* 20.

References

Baade, W. & Minkowski, R., 1954. *Astron. J.*, **119**, 206.
Briggs, B. H., 1958a. *J. Atmos. Terr. Phys.*, **12**, 34.
Briggs, B. H., 1958b. *J. Atmos. Terr. Phys.*, **12**, 89.
Briggs, B. H. & Spencer, M., 1954. *Rep. Prog. Phys.* **17**, 245.
Chivers, H. J. A., 1960. *J. Atmos. Terr. Phys.* **19**, 54.
Dagg, M., 1957. *J. Atmos. Terr. Phys.*, **10**, 204.
Fejer, J. A., 1953. *Proc. Roy. Soc. A.*, **220**, 455.
Harrower, G. A., 1957a. *Canad. J. Phys.* **35**, 512.
Harrower, G. A., 1957b. *Canad. J. Phys.* **35**, 522.
Hewish, A., 1951. *Proc. Roy. Soc. A.*, **209**, 81.
Hewish, A., 1952. *Proc. Roy. Soc. A.*, **214**, 494.
Jennison, R. C. & Latham ,V., 1959. *Mon. Not. Roy. Astron. Soc.*, **119**, 174.
Jones, I. L., 1960. *J. Atmos. Terr. Phys.*, **19**, 26.
Koster, J. R. & Wright, R. W., 1960. *J. Geophys. Res.*, **65**, 2303.
Little, C. G. & Maxwell, A., 1951. *Phil. Mag.*, **42**, 267.
Lyon, A. J., Skinner, N. J. & Wright, R. W. H., 1960. *J. Atmos. Terr. Phys.*, **19**, 145.
Ryle, M. & Hewish, A., 1950. *Mon. Not. Roy. Astron. Soc.*, **110**, 381.
Shimazaki, T., 1959a. *J. Radio Res. Labs.*, **6**, 669.
Shimazaki, T., 1959b. *J. Radio Res. Labs.*, **6**, 688.
Spencer, M., 1955. *Proc. Phys. Soc.*, **B68**, 493.
Wright, R. W., Koster, J. R. & Skinner, N. J., 1956. *J. Atmos. Terr. Phys.*, **8**, 240.

Preliminary Palaeomagnetic Measurements on Silurian Sediments from South Africa

K. W. Graham and A. L. Hales

(Received 1961 March 16)*

Summary

This paper describes palaeomagnetic measurements made on the Lower "Shales" of the Table Mountain Series, near Cape Town. The age of this formation is probably Silurian. Samples collected at the surface were found to be inconsistently magnetized, but those from a fine red mudstone bed exposed in a deep road cutting gave consistent results. Eight samples from this bed give a mean direction of $D = 341°{\cdot}8$. $I = 3°{\cdot}5$ with the south pole downwards.

1. Introduction

Considerable difficulties have been found in interpreting palaeomagnetic measurements on surface samples of South African rocks. It is thought that a major part of the difficulty in interpretation arises from the remagnetization of near surface samples by the magnetic fields associated with lightning currents (Graham, submitted for publication). At depth these difficulties do not arise and significant results have been obtained. (Gough 1956, Graham & Hales 1957).

Many of the significant results obtained elsewhere were from samples of red sandstones and shale. For this reason an extensive sampling programme was carried out on the red sandstones and mudstones on the slopes of Chapman's Peak near Cape Town.

These sediments are known as The Lower Shales of the Table Mountain Series of the Cape System.

2. The age of the Cape system

The Palaeozoic "Cape System" of South Africa has the subdivisions:

Witteberg Series
Bokkeveld Series
Table Mountain Series.

The Witteberg Series contains occasional plant fossils of Devono–Carboniferous affinities. The Bokkeveld Series contains abundant marine fossils of Devonian age. Since no identifiable fossils have been found in the Table Mountain Series, its

* Received in original form 1960 January 21.

age must be inferred from that of the Bokkeveld Series. Du Toit (1954) regards the T.M.S. as "certainly not younger than the Lower Devonian", and a Silurian age is generally ascribed to this formation.

3. The sampling

In the first sampling a number of hand samples and 6-in cores were collected from the Lower "Shales" of the Table Mountain Series at Chapman's Peak (Lat. 33°·1 S. Long. 18°·3 E.) near Cape Town. The directions of magnetization of these samples are shown in Figure 1(a). It was thought that the near-random patterns of magnetization of the first set of samples might be due to slight weathering, or thermo-stress cycling of the outermost few inches of the outcrop and that more consistent results might be obtained if deeper samples were obtained. Accordingly a portable drill rig was developed with which oriented cores could be obtained to a depth of three feet. (Graham & Keiller 1960).

Using this rig, 46 3-ft cores were drilled from rock exposed in a deep road cutting as well as on the mountain side below the cutting. Some of the cores were drilled upwards or downwards at small angles to the horizontal so as to pass very slowly through a few inches of the untilted sediments. Other cores were drilled at steeper angles to sample two feet or more of the geological column. Figure 2 shows diagramatically the relative positions of the various boreholes and the vertical thickness of sediment represented by each of the 3-ft cores. The portion of this diagram above the dotted line represents the road cutting while that below the dotted line represents the steep mountain side. The wall of the road cutting from which the samples were drilled is about 50 ft to the south east of the natural cliff and almost parallel to it.

4. The samples from the cutting

Three pairs of cores were drilled about fifty feet apart so as to intersect exactly the same few inches of a red siltstone bed about two feet thick. Another core (39) was drilled so as to cut the entire bed. Core No. 10 also came from this bed. Other cores were drilled from the almost glassy quartzite exposed in the road cutting above and below the fine grained bed.

The directions of magnetization of the samples from the red siltstone in the cutting are extremely consistent both laterally over the 100 ft sample as well as over its thickness. As examples, the directions of magnetization of cores 17, 39 and 19 are plotted stereographically (on the lower hemisphere) as Figures 1 (b), (c) and (d). The mean directions of magnetization of the mudstone cores, are given in Table 1. The semi-angles of the cones of 95 per cent confidence (α) were calculated by Fisher's method (Fisher 1953) and are also given in Table 1. The mean direction of magnetization of this layer, giving each core unit weight, is declination 341°·8, inclination 3°·5 with a South pole downwards. The semi-angle of the cone of 95 per cent confidence (α) is 4°·5.

The quartzite above and below shows considerable scatter in the directions of magnetization of the specimens from each core, but qualitatively the directions are not inconsistent with those from the fine grained bed as may be seen from Figure 1(e) and 1(f).

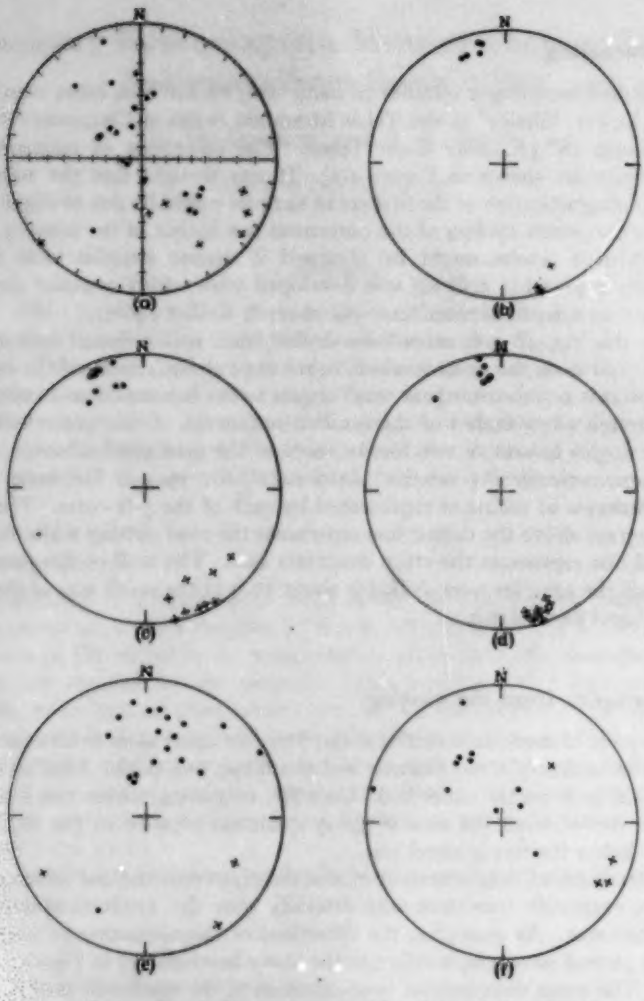

FIG. 1.—Lower hemisphere stereographic plots of the directions of magnetization of (a) the reconnaissance samples; (b) to (f) the specimens from cores 17, 39, 19, 43 and 48 respectively.

● = South pole downwards × = North pole downwards.

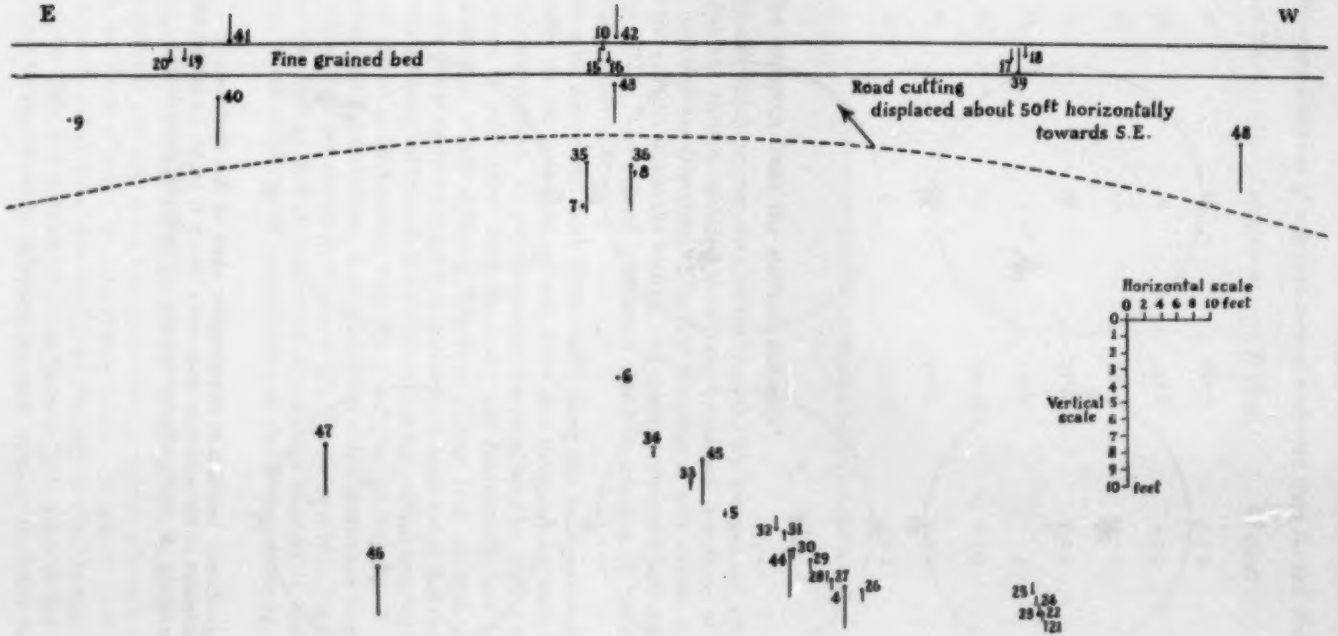

FIG. 2.—A diagrammatic representation of the vertical and horizontal distances between the Cape sample sites and the length of the geological column covered by each bore core.

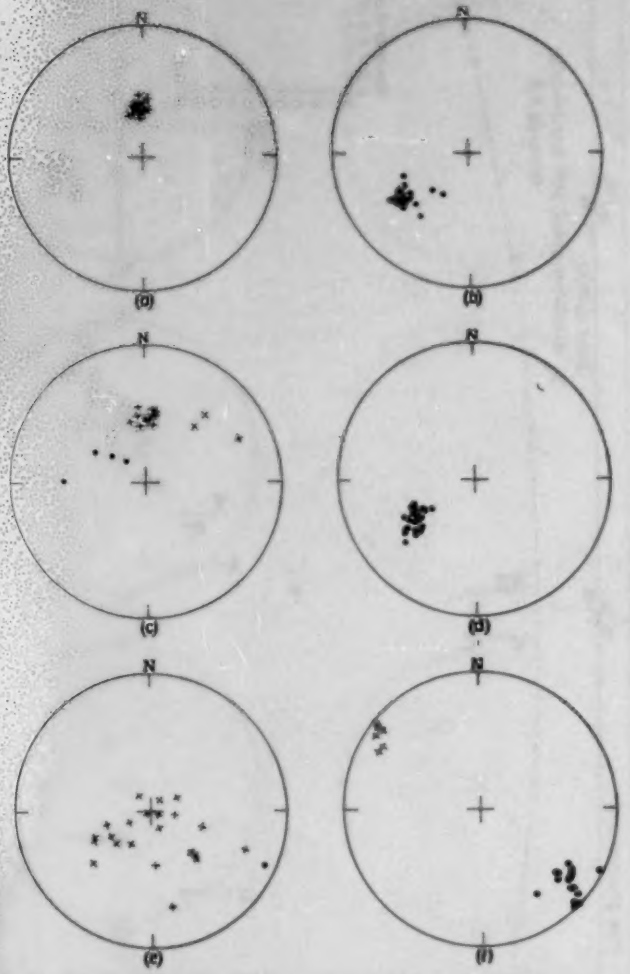

FIG. 3.—Lower hemisphere stereographic plots of the directions of magnetization of the specimens from cores Nos. 7, 8, 35, 36, 44 and 46 respectively. ● South pole downwards; × North pole downwards.

Table 1

The mean directions of magnetization of each core from the red, fine grained bed

Core No.	No. of specimens	D (deg)	I^* (deg)	α (deg)
10	18	341·7	+5·2	4·5
15	10	345·6	+9·2	6·4
16	10	342·3	+7·9	5·5
17	8	341·8	+2·0	5·7
18	7	332·7	−1·5	5·7
19	15	344·6	+1·6	5·4
20	22	349·7	+2·9	2·8
39	17	335·8	+0·2	6·2

* A positive inclination indicates a South pole downwards.

5. The samples from the surface outcrop

Broadly speaking, the cores drilled from the fine grained red, arkosic sandstone forming the surface outcrops show two prominent directions of magnetization with intermediate directions. The first direction is very similar to that obtained from the samples inside the cutting, and consists of almost horizontal South poles to the NNE. The second prominent direction consists of North poles nearly vertically downwards.

Samples distributed both horizontally along the same sedimentary layer and vertically up the geological column show that these surface outcrops are inconsistently magnetized. In one spectacular instance, samples Nos. 7 and 8, although very close to each other both vertically and horizontally (see Figure 2, were magnetized in widely differing directions. Cores Nos. 35 and 36 were drilled vertically above numbers 7 and 8 respectively, in such a way that each would cover the material sampled by both 7 and 8 as well as the vertical interval between them. No. 35 agreed in its direction with No. 7 and No. 36 with No. 8. Stereographic projections of the directions of magnetization of the specimens from each of cores 7, 8, 35 and 36 are shown in Figure 3 (a), (b), (c) and (d). Figure 3(e) and (f) represents cores 44 and 46 and serves as a further example of horizontal inconsistency in the directions of magnetization of the surface outcrops.

6. Discussion

Since the directions of magnetization of the surface outcrop cores from the same horizons and only a few feet apart differ so widely, it is clear that some local cause has been effective in magnetizing them. It follows that the measured directions do not give any meaningful information on the direction of the Earth's field at the time of deposition of the sediments. It is possible that the specimens have been remagnetized by lightning currents running down the cliff towards the sea.

On the other hand, allowing for the expected poor grouping of the directions of magnetization of the coarse grained quartzites, samples collected from a deep road cutting are consistently magnetized. Although secular variation may not have been meaned out completely, it seems probable that the mean direction of magnetization of the red, fine grained bed is a reasonable approximation to the direction of the field during Silurian times.

Assuming an axial dipole field, the South pole relative to Africa would have the present-day coordinates of longitude 10°·9 W, latitude 50°·3 N (or the North Pole 169°·1 E, 50°·3 S). The co-latitude of the Cape Peninsula relative to this Silurian pole would be 88°, which places South Africa very nearly on the equator at that time. The presence of a tillite in the Upper T.M.S. Shales is puzzling and demands further work on the Cape System.

It is interesting to compare this pole position with those found for other continents. Figure 4 is based on Cox and Doell's Figure 23 (Cox & Doell 1960) and

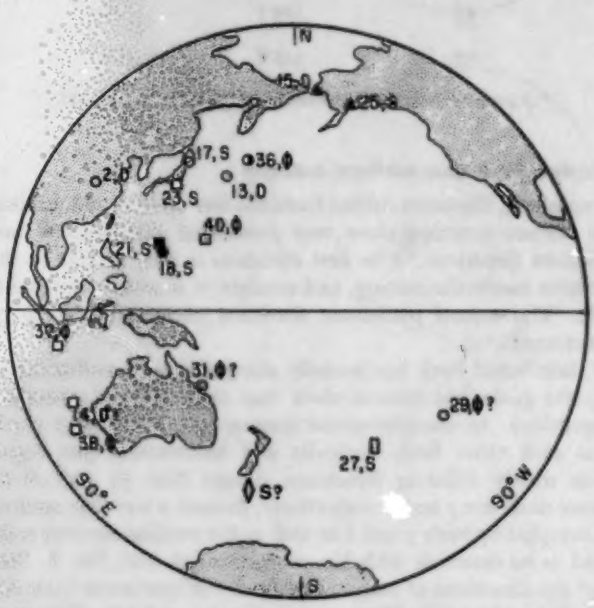

FIG. 4.—Early Palaeozoic Virtual Geomagnetic Poles (after Cox and Doell 1960, Figure 23). The numbers and symbols are those used by Cox and Doell.

○ European	D = Devonian
□ North American	S = Silurian
△ Australian	φ = Ordovician
▯ Asian	● = South magnetic poles
◇ African	○ = North magnetic poles

◑ = Poles from measurements with mixed polarity.

shows clearly that the pole position found from the Lower Shales of the Table Mountain Series is not in agreement with those of Ordovician, Silurian or Devonian age from any of the other continents.

7. Acknowledgments

It is a pleasure to acknowledge our indebtedness to Dr A. Fuller of the Geology Department of the University of Cape Town for much helpful advice and criticism in connection with this work. We are also indebted to the Council of Scientific and Industrial Research for a grant for this work.

Bernard Price Institute of Geophysical Research,
University of the Witwatersrand,
Johannesburg, South Africa.
1961 *January.*

References

Cox, A., & Doell, R. R., 1960. *Bull. Geol. Soc. Amer.*, **71**, 645.
Du Toit, A. L., 1954. *Geology of South Africa*, 3rd Edition, Oliver and Boyd.
Fisher, R. A., 1953. *Proc. Roy. Soc. A.*, **217**, 295.
Gough, D. I., 1956. *Mon. Not. R. Astr. Soc. Geophys. Suppl.*, **7**, 196.
Graham, K. W. T., & Hales, A. L., 1957. *Phil. Mag. Suppl.*, **6**, 149.
Graham, K. W. T., & Keiller, A. B., 1961 (in press).

Book Review

Infra-red Physics

Volume 1, No. 1, 1961

(Pergamon Press. Quarterly, annual subscription £7.)

Infra-red Physics, published by Pergamon Press, has given your reviewer experience of the razor-edge of ambivalence. There is pleasure that this publicly neglected subject has a Journal of its own, horror that yet another journal must be purchased by libraries and scanned by readers. There is delight in the progress of the subject over the last decade; regret at its regressions.

Wild surmise greeted the announcement by Hanbury-Brown and Twiss of the positive result of their famous experiment on photon-correlation. This shows how teaching still largely neglects both physical statistics and infra-red physics. The worker in infra-red (which is our present concern) is daily confronted with the wave-particle duality, because the infra-red spectrum spans the transition from the Rayleigh-Jeans realm of microwaves to the classical-particle statistics of the optical region. It has therefore a special claim to the attention of students of fundamental physics.

Volume 1 of the *Journal* opens with an historical paper on Sir William Herschel. There is a welcome review article on infra-red detectors. A number of articles describe devices; these include sources for communication, tellurium detectors, germanium dioxide glasses, interference modulation of millimetre waves, a sun-seeker, phophor photography, absorption-edge thermal imaging, and a scanning Fabry–Perot. There is a research note on absorption in lead halides.

A notable advance, as compared with the literature of 10 years ago, is the universal use of physical units of detectivity. The days of standardization by cigarette ends, soldering irons and signal school black have passed unmourned.

A regression is that particle-statistical approximations, using crude estimates of effective wavelength, have often replaced the more exact formulae for ultimate sensitivity. The term "ultimate sensitivity" is due to Jones (1947), and "detectivity" was suggested by your reviewer (Jones, 1952). "Ultimate sensitivity and practical performance" is a direct quote from the reviewer (Fellgett 1949), who is disappointed that the article under this title did not use, or refer to, the more exact formulae for estimating these quantities, which it is now believed have been correctly extended to non-equilibrium conditions (Fellgett, Jones & Twiss, 1959). The loss of accuracy is small at present, but the loss of insight is great.

Science has so far made relatively little use of the powerful conceptual and technical methods now available for the creation, copying, and retrieval of documents. Each new journal raises the question of how long conventional publication can continue to be a major method of scientific communication. There are cheaper means of creating easily-read text than by printing, and more effective means of search than by using subject-indices or scanning the pages of a journal devoted

to a particular aspect of science. Yet the prestige and unity of a published paper have an irreplaceable value. Refereeing contributes essentially to this value, but may make it easier to publish a mediocre paper than either a very bad or a very good one. An author who fails to place his manuscript with one journal can try elsewhere, and in this way can obtain an assessment which is disinterested, and is seen to be so. Unified publication is unacceptable because it would destroy this freedom.

As science expands, new journals are needed. But if their number continues to multiply unchecked, the whole system may break down. The obligations of libraries have the effect of blunting economic selection. Some curb must be found, and it must be closely related to the exploitation of new techniques of scientific communication.

PETER FELLGETT

References

Jones, R. C., 1947. *J. Opt. Soc. Amer.*, **37**, 879.
Jones, R. C., 1952. *Nature* (*London*), **170**, 937.
Fellgett, P. B., 1949. *J. Opt. Soc. Amer.*, **39**, 970.
Fellgett, P. B., Jones, R. C., & Twiss, R. Q., 1959. *Nature* (*London*), **184**, 967.

Geophysical Journal

RECOMMENDATIONS TO AUTHORS

1. Authors are advised to follow the general suggestions for the preparation of scientific papers given in *Notes on the preparation of papers to be communicated to the Royal Society* and in *The printing of mathematics* by T. W. Chaundy, P. R. Barrett and C. Batey (Oxford University Press, 1954). In particular the abbreviations for the names of periodicals used in the *Geophysical Journal* are those given in *Notes on the preparation of papers . . .* and the symbols, signs and abbreviations are those recommended for British scientific publications by the Symbols Committee of the Royal Society.

2. Papers should be typewritten with double spacing and on one side of the paper only. Two copies, one of them the top copy, should be submitted. All papers must be accompanied by a summary; summaries are not required for *Letters to the Editors*.

3. Tables are printed without rules. They should be numbered serially with Arabic numerals. Table headings should be brief. Units should be placed at the head of the column. Tables should be typed on separate sheets and their positions in the text indicated on the copy.

4. Illustrations, especially photographs, should be kept to a minimum, and the same information should not in general be given in both tables and illustrations. Line drawings should be in dense black ink on smooth white board or transparent tracing film. Original drawings must not be lettered; lettering should be indicated on copies or photoprints which must be supplied in addition to the originals. Wherever possible, lettering should be kept outside the diagram so that it may be set in type. Diagrams should be drawn at twice to three times the size at which they will be printed. The maximum dimensions for diagrams, when reduced and with their lettering and captions, are 8 in by 5 in. A wide variety of flat tints of dots, lines and shadings can be applied to line drawings by the blockmaker. Photographs for reproduction should be unmounted glossy prints and should be accompanied by lettered prints.

5. References should be quoted in the form recommended by the Royal Society but authors may also quote titles of papers if they wish. References in the text are made in the form (Smith 1940).

6. Authors whose work involves much mathematics should follow carefully the recommendations in *The Printing of Mathematics*.

7. The Editors will be glad to advise authors on any special points of difficulty arising in the preparation of papers for the *Journal*.

Contents

PAGE

K. F. Bowden & P. Hughes, The flow of water through the Irish Sea and its relation to wind 265

K. Aki & F. Press, Upper mantle structure under oceans and continents from Rayleigh Waves 292

B. H. Briggs, The correlation of radio star scintillations with geomagnetic disturbances 306

K. W. Graham & A. L. Hales, Preliminary palaeomagnetic measurements on Silurian sediments from South Africa 318

Book Reviews 326

Printed in Great Britain by J. W. Arrowsmith Ltd., Bristol